國立交通大學

應用化學系

碩士論文

利用熱力學方法探討

半導體材料的熱電效應

Thermodynamic Study of the

Thermoelectric Effect for

Semiconducting Materials

研究生：蔡琇雅

指導教授：朱超原 博士

中華民國九十八年一月

利用熱力學方法探討

半導體材料的熱電效應

Thermodynamic Study of the
Thermoelectric Effect for
Semiconducting Materials

研究生：蔡琇雅   Student: Hsiu-Ya Tsai

指導教授：朱超原   Advisor: Chaoyuan Zhu

國立交通大學

應用化學系

碩士論文

A thesis

Submitted to Department of Applied Chemistry

College of Science

National Chiao Tung University

in Partial Fulfillment of the Requirements

for the Degree of Master

November 2008

Hsinchu, Taiwan

中華民國九十八年一月

利用熱力學方法探討
半導體材料的熱電效應

研究生 ： 蔡琇雅　　　　指導教授 ： 朱超原

國立交通大學應用化學系

摘要

　　半導體材料的熱電效應可以藉由熱力學方法中 ： 一系統存在電場的情況下，而詳加研究。併入 Clausis-Mossotti 方程式的這個新的方法被提出來計算固態材料的介電常數，然後便可以計算出一個決定材料熱電轉換效率的重要因子 ： 熱電係數。

　　一般來說，在 Clausis-Mossotti 方程式中的極化率包含三個部份 ： 電子極化率、原子極化率與方向性極化率，然而對於半導體材料的主要貢獻來自於電子極化率。從極化率得到的介電常數因為擁有粒子聚集的重要巨觀特性，因此，從電子極化率衍生而來的介電常數便可以將此巨觀特性描述為一個固態性質。Ab initio 量子化學的理論被運用在計算隨著電場變化的電子極化率之上。

　　在目前的工作中，三種半導體的熱電材料被考慮 ： 矽化鎂、二矽化鐵和矽化鍺。第一步，APT 和Mulliken電荷經由密度泛涵理論的方法在一變化的電場下而計算出來，變化的電場如下 ： -0.01、-0.0075、-0.005、-0.0025、0.00、0.0025、0.005、0.0075 和 0.01 原子單位。四種密度泛涵理論的方法被選用，如下 ：B3LYP、BLYP、M05 和M052X，再加上一系列的基底函數，如下 ：Pople形式的基底函數，例如 6-311G、6-311G(d)⋯等等 ； effective core potential形式

的基底函數，例如CEP-31G、CEP-121G和LANLDZ。第二步，APT和Mulliken電荷被使用來計算在電場中的偶極矩，然後電子極化率可經由偶極矩對電場求一階導數而計算出來。最後，介電常數便可以從Clausis-Mossotti方程式與電子極化率而求得。經與實驗測量比較之下，對於矽化鎂、二矽化鐵和矽化鍺而言，在B3LYP方法之下所模擬計算出來的介電常數顯示最正確的結果。介電常數從目前的計算方法及他們相對應的實驗結果，分別如下：對於矽化鎂而言，ε_r = 11.86 和 13.3 ；對於矽化鐵而言，ε_r = 27.806 和 27.6 ；對於矽化鍺而言，ε_r = 13.571 和 13.95。

熱電係數可以從熱力學方法中的chemical potential計算求得，這種方法比能帶結構理論還簡單的多。Helmholtz自由能在不同溫度下被計算，而且基於溫度為一變量之下，可以得到某些分析性的函數。因此，熱電係數可經由Helmholtz自由能對溫度求一階導數而計算出來。然而，這個熱電係數還要除以先前計算的介電常數，最後才能真正表示固態材料的熱電係數。對於熱電係數而言，目前計算矽化鎂、二矽化鐵和矽化鍺的結果與實驗測量的結果非常相近。經由目前計算的熱電係數，分別如下：矽化鎂在溫度(300, 800)K下，S_e = (284,334) μV/K ；二矽化鐵在溫度(300,900)K下，S_e = (118.8,140.4) μV/K ；矽化鍺在溫度(300, 900)K下，S_e = (196.3,220.9)。與之相對應的實驗結果，分別如下：矽化鎂在溫度(300, 800)K下，S_e = (180,280) μV/K；二矽化鐵在溫度(300, 900)K下，S_e = (190, 170) μV/K；矽化鍺在溫度(300, 900)K下，S_e = (345,325) 。

總之，對於計算熱電係數而言，目前計算的方法明顯優於傳統能帶結構理論的方法。

Thermodynamic Study of the Thermoelectric Effect for Semiconducting Materials

Student: Hsiu-Ya Tsai   **Advisor: Chaoyuan Zhu**

Department of Applied Chemistry

National Chiao Tung University

Abstract

Thermoelectric effect of semiconducting materials is studied by the thermodynamic method for a system in the presence of an electric field. The new method incorporating with the Clausis-Mossotti equation is proposed to calculate dielectric constant for solid-state materials, and then to compute the Seebeck coefficient that is key factor to determine thermoelectric conversion efficiency of the materials.

The polarizability in the Clausis-Mossotti equation in general includes three parts; electronic polariability, atomic polariability and orientation polariability. The dominant contribution for semiconducting materials comes from electronic polariability. A dielectric constant derived from the polarizability is an important bulk property of a collection of particles. Therefore, the dielectric constant derived from electronic polariability can describe bulk as a solid. Ab initio quantum chemistry theory is utilized to compute electronic polariability directly with

varying strength of electric field.

In the present work, three semiconductor thermoelectric materials are considered; Mg2Si, FeSi2 and SiGe. In the first step, APT and Mulliken charges are computed with density functional theory (DFT) method at various electric fields; -0.01, -0.0075, -0.005, -0.0025, 0.00, 0.0025, 0.005, 0.0075 and 0.01 in atomic unit. Four kinds of DFT functionals are chosen: B3LYP, BLYP, M05 and M05-2X, plus a bunch of basis sets; Pople style basis sets including of 6-311G, 6-311G(d)…etc; effective core potential including of CEP-31G, CEP-121G and LANL2DZ. In the second step, APT and Mulliken charges are used to calculate dipole moments at given electric field above and then derivatives of dipole moments with respect to electric field lead to the electronic polarizability. In the final step, the dielectric constant is evaluated from the Clausis-Mossotti equation through the electronic polarizability. In comparison with experimental measurements, simulated dielectric constants with B3LYP method show the most accurate results for Mg2Si, FeSi2 and SiGe. The dielectric constants from the present calculations and their corresponding experiment results are ε_r = 11.86 and 13.3 for Mg_2Si, ε_r = 27.806 and 27.6 for $FeSi_2$, and ε_r = 13.571 and 13.95 for SiGe, respectively.

The Seebeck coefficient is calculated from the thermodynamic method with chemical potential. This method is much simpler than energy band structure theory. The Helmholtz free energies are computed at various temperatures, and then are fitted into the certain analytical function with respect temperatures as a variable. Thus, the Seebeck coefficient can be evaluated from partial derivative of Helmholtz free energy with respect to temperature. This Seebeck coefficient that must be divided by the dielectric constant evaluated previously can finally be

considered as the Seebeck coefficient for a solid-state material. The present results show good agreements with experimental measurements for the Seebeck coefficients of Mg2Si, FeSi2 and SiGe. The Seebeck coefficients from the present calculations are $S_e = (284, 334)\mu V/K$ at the temperature (300, 800)K for Mg_2Si, $S_e = (118.8, 140.4)\mu V/K$ at (300,900)K for $FeSi_2$, and $S_e = (196.3,220.9)\mu V/K$ at (300,900)K for SiGe. Their corresponding experiment results are $S_e = (180, 280)\mu V/K$ at (300, 800)K for Mg_2Si, $S_e = (190, 170)\mu V/K$ at (300,900)K for $FeSi_2$, and $S_e = (345,325)\mu V/K$ at (300,900)K for SiGe.

In conclusion, the present method surprisingly woks better than conventional energy band structure theory for calculating the Seebeck coefficient.

Acknowledgments

There are so many people that have helped me on the path to my Master's degree. Firstly, I must offer my deep thanks to my advisor, Prof. Zhu. He accepted me as his student when I was about to second grade of graduate school, no matter how I wasn't familiar with the field of computational chemistry. He taught me the base of quantum chemistry and computational chemistry one on one, like a tutor. Those made me handle the job soon, and he gave me a lot of suggestions when I met some difficulties on my research. The most importance is that I discovered the interests of doing researches from his teaching. Secondly, I thank my family, especially for my mother, she tried to give me a much healthier family, and paid her all love and care to our three children. Thirdly, I thank my boy friend that always hears my arguments quietly for everything, no matter it is good or bad, and comforts me and encourages me at the right moment. Finally, I also thank everyone who has ever helped me, like oral committee members including Prof. 李積琛, 林聖賢 and 陳煜璋 who make my thesis more complete; my rootmats including 鈺君, 春慧 and 小莫 who let me experience a crazy life during staying in dorm; 靜怡 who always shares anything no matter about research knowledge or life information with me; 雅利, Amy, 何榮幸, 彭亮…etc. I am very happy for studying in the department of applied chemistry, and those days I stayed in school I never forget it.

Contents

List of Figures

List of Tables

Chapter 1 Introduction

Recently Greenhouse effect is more serious and it speeds up the research for the alternative sources of energy in place of traditional fossil fuels. Power generation from the solar energy has attracted more attention, but it is still insufficient for the current huge energy consumption. Thermoelectric materials have the property for recovering the wasting heat to generate useful electric power and for reducing global warming effects. Since this energy conversion is done by electron moving in solid, we can make full use of solid. Firstly, the thermoelectric device has no moving part, and is operated almost without the maintenance. Besides, thermoelectric energy conversion has several advantages in comparison with the other energy sources. Secondly, it produces no waste matter through conversion process. Thirdly, it can be processed at a micro/nano size, and can be implemented into electronic devices[1].
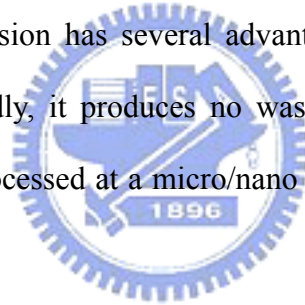
The efficiency of energy conversion for a thermoelectric material is measured by the dimensionless thermoelectric figure of merit, written as ZT, and it is defined by

$$ZT = \frac{S_e^2 \sigma T}{k_{phonon} + k_{electron}} \tag{1.1}$$

where S_e is Seebeck coefficient, σ is the electrical conductivity, k_{phonon} and $k_{electron}$ are the thermal conductivity for the phonon and the electron respectively, and T is temperature. The ideal thermoelectric material would have a large S_e, a large σ and a small k. For an insulator it usually has a large S_e and a small k, but it has a small σ, while for a metal it has a large S_e and σ, but it has a large k. Therefore, how to

enhance ZT for thermoelectric materials is a very challenging problem, because material with a large σ is usually companied with a small S_e and a large k. The trade off between the electrical conductivity and Seebeck coefficient can be seen in Fig. 1[2] for bulk silicon crystals[2].
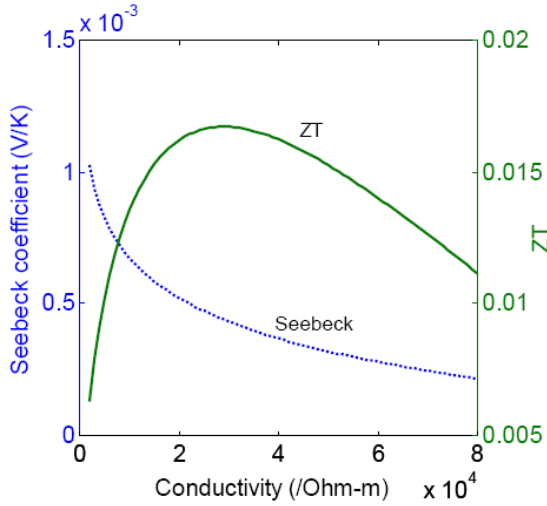
Fig. 1   Seebeck coefficient and ZT as a function of the electrical conductivity for bulk crystal Silicon at 373K[2].

If ZT goes to zero, it means there is no energy conversion. But as ZT is increasing to infinity, it will reach the Carnot efficient limit, which applies to all heat engines[3]. The laws of thermodynamics tell us that a maximum efficiency, called the Carnot efficiency, cannot be exceeded. The Carnot efficiency can be written

$$\eta = \frac{T_{Hot} - T_{Cold}}{T_{Hot}} \times 100\% \tag{1.2}$$

where T_{Hot} and T_{Cold} are the temperatures of the hot and cold sides of the materials.

The comparison of ZT values with different materials can be seen in Fig. 2[4], where the most of materials are located below ZT=1. Non-oxide materials have

large ZT values and oxide materials have small ZT values, and the ZT values of SiGe crystals approach to 1, and the ZT values of β-FeSi2 is between 0.1 and 1.
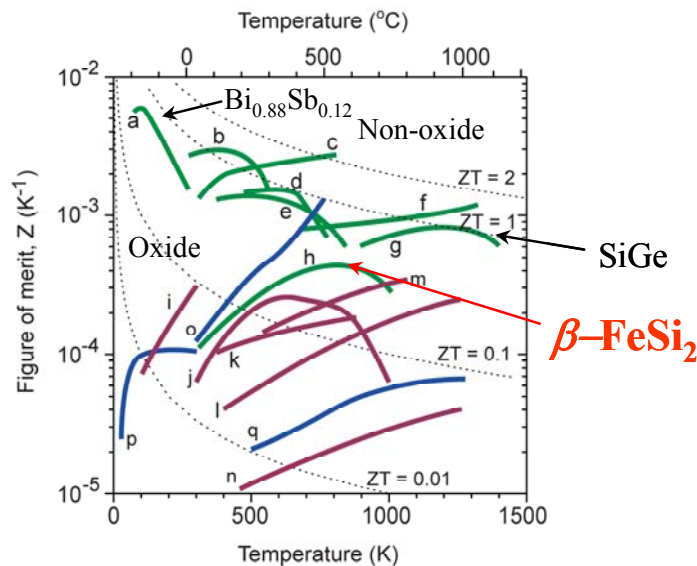
Fig. 2   The comparison of ZT values from different materials[4].
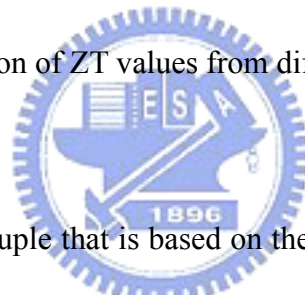
The traditional thermocouple that is based on the two dissimilar metal wires is for the first time to apply for thermoelectrics. From the 1950s the semiconductors replaced the metals and especially in the 1990s the research of thermoelectric materials achieved the big progress[3] and it can be demonstrated in Fig. 3[5]. The research for thermoelectric silicide materials is grouped into two categories; one is alkaline-earth metal silicides and the other is transition metal disilicide. Magnesium silicide Mg_2Si that is n-type semiconductor is widely used for the application to the thermoelectric devices, as it is abundant in the natural resources, besides it is non-toxic, inexpensive. Mg2Si is the well known promising thermoelectric material in temperature range from 500 to 800K[6] and with narrow-band gap about 0.78 eV[7]. β-FeSi2 is another promising thermoelectric material according to its energy band gap, thermal stability and corrosion resistance[6]. It is mainly used for generating

power in the temperature range from 500 too 900K[6].
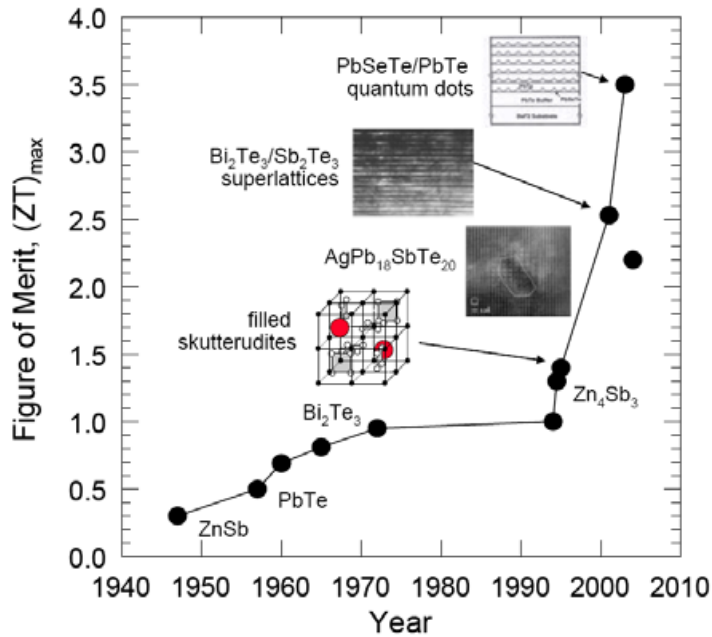
Fig. 3　Progress in thermoelectric materials figure of merit, ZT.

The Seebeck coefficient that is also called as thermopower is the important parameter to determine the thermoelectric conversion efficiency of thermoelectric materials and its magnitude depends on an induced thermoelectric voltage across the materials in response to a temperature difference. The Seebeck coefficient is usually calculated from the charge carrier motion of energy band gap, because an applied temperature difference will cause charge carriers (electrons or holes) in the materials to diffuse from the hot side to the cold side. As diffusions of charge carriers reach thermodynamic equilibrium, the net separation of carriers would create an electric potential. However, phonons are not always in local thermal equilibrium. They lose momentum by interacting with other carriers and tend to push electrons to one side of the materials. So the Seebeck coefficient is mainly affected by the following two reasons: charge carrier diffusion and phonon drag.

However, diffusing charge carriers would also be scattered by impurities, defects, phonons and other charge carriers, etc[8]. The above factors complicate the calculations of the Seebeck coefficient considerably in the conventional band structure theory.

We have found an alternative way to study the thermoelectric dynamics. It is based on the thermodynamic theory for the system in equilibrium with an electric field. As thermodynamics is considered as an exact theory in which all microscopic quantities can be averaged out systematically, it is possible to perform a more accurate calculation[9].

In the present work, three semiconductor thermoelectric materials, Mg2Si, FeSi2 and SiGe, were investigated. In the first step, APT and Mulliken charges are computed with density function theory (DFT) method at various electric fields. Four DFT functionals are chosen; B3LYP, BLYP, M05 and M05-2X. In the second step, APT and Mulliken charges are used to calculate dipole moments at a given electric field and then derivatives of dipole moments with respect to electric field lead to the electronic polarizability. In the final step, the dielectric constant is evaluated from the Clausis-Mossotti equation through the electronic polarizability.

The Seebeck coefficient is calculated from the thermodynamic method with chemical potential. This method is much simpler than energy band structure theory. The Helmholtz free energies are computed as a function of the temperature, and then are fitted into an analytical function with respect temperatures as a variable. Seebeck coefficient can be evaluated from partial derivative of Helmholtz free energy with respect to temperature, which is divided by dielectric constant evaluated previously and finally be considered as the Seebeck coefficient for a solid-state material. Some experimental data are included in the present method, for

example, the density of the material[9].

Chapter 2 Theory

2-1 The Electric Properties of Matter

2-1-1 Basic relation of electric field, energy and polarizability

There exist both time-dependent and the time-independent electric fields. Time-dependent field is usually associated with electromagnetic radiation characterized by a frequency of implying dynamic properties, while time-independent field does not vary with accompanying frequency of implying static properties. The present work is focused on the static electric field that is also called the homogeneous electric field here[10].

In the presence of a homogeneous external electric field, the Hamiltonian for the total system (nuclei and electrons) can be written as[11]

$$\hat{H} = \hat{H}^{(0)} + \hat{H}^{(1)} \tag{2.1}$$

where $H^{(0)}$ is unperturbed term without the field for the system and $H^{(1)}$ has the form

$$\hat{H}^{(1)} = -\hat{\mu}_x F_x - \hat{\mu}_y F_y - \hat{\mu}_z F_z = -\hat{\mu} \cdot F \tag{2.2}$$

in which the dipole moment operator μ is given by

$$\hat{\mu} = \sum_i q_i r_i \tag{2.3}$$

with the vector r_i indicating the particle i with charge q_i

From eq. (2.1) and (2.2) it can be obtained the relation,

$$\frac{\partial \hat{H}}{\partial F_a} = -\hat{\mu}_a \qquad a \in x, y, z \tag{2.4}$$

From eq. (2.4) it follows
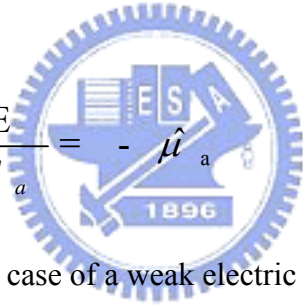
$$\left\langle \psi \left| \frac{\partial \hat{H}}{\partial F_a} \psi \right. \right\rangle = -\left\langle \psi \left| \hat{\mu}_a \psi \right. \right\rangle = -\hat{\mu}_a \tag{2.5}$$

where μ_a is the expectation of the a-th component of the dipole moment

From the Hellmann-Feynman theorem it follows

$$\left\langle \psi \left| \frac{\partial \hat{H}}{\partial F_a} \psi \right. \right\rangle = \frac{\partial E}{\partial F_a} \tag{2.6}$$

therefore

$$\frac{\partial E}{\partial F_a} = -\hat{\mu}_a \tag{2.7}$$

Moreover, if it is in the case of a weak electric field **F**, it can be written as the Taylor expansion at **F** = 0.

$$E(F) = E^{(0)} + \sum_a \left(\frac{\partial E}{\partial F_a} \right)_{F=0} F_a + \frac{1}{2!} \sum_{a,a'} \left(\frac{\partial^2 E}{\partial F_a \partial F_{a'}} \right)_{F=0} F_a F_{a'}$$
$$+ \frac{1}{3!} \sum_{a,a',a''} \left(\frac{\partial^3 E}{\partial F_a \partial F_{a'} \partial F_{a''}} \right)_{F=0} F_a F_{a'} F_{a''} + \dots \qquad a,a',a'' \in x,y,z \tag{2.8}$$

where $E^{(0)}$ is the energy of the unperturbed term for the system.

Combining eq. (2.7) with (2.8), we can have

$$\frac{\partial E}{\partial F_a} = -\hat{\mu}_a = \left(\frac{\partial E}{\partial F_a} \right)_{F=0} + \sum_{a'} \left(\frac{\partial^2 E}{\partial F_a \partial F_{a'}} \right)_{F=0} F_{a'}$$
$$+ \frac{1}{2} \sum_{a'} \left(\frac{\partial^3 E}{\partial F_a \partial F_{a'} \partial F_{a''}} \right)_{F=0} F_{a'} F_{a''} + \dots \tag{2.9}$$

In terms of the derivatives in eq. (2.9), the permanent dipole moment, the polarizability and the (first) hyperpolarizability

$$\mu_a = \mu_a^{(0)} + \sum_{a'} \alpha_{a,a'} F_{a'} + \frac{1}{2} \sum_{a',a''} \beta_{a,a',a''} F_{a'} F_{a''} + ...$$ (2.10)

The meaning of the formula for μ_a is listed :

the total dipole moment (field-dependent) :

$$\mu_a = -\frac{\partial E}{\partial F_a}$$ (2.11)

the permanent (field-independent) dipole moment :

$$\mu_a^{(0)} = -\left(\frac{\partial E}{\partial F_a}\right)_{F=0}$$ (2.12)

the component aa' of the polarizability tensor :

$$\alpha_{a,a'} = -\left(\frac{\partial^2 E}{\partial F_a \partial F_{a'}}\right)_{F=0} = \left(\frac{\partial \mu_a}{\partial F_{a'}}\right)_{F=0}$$ (2.13)

the component aa'a'' of the (first) hyperpolarizability tensor :

$$\beta_{a,a',a''} = -\left(\frac{\partial^3 E}{\partial F_a \partial F_{a'} \partial F_{a''}}\right)_{F=0}$$ (2.14)

In other words, an induced dipole moment, which consists of the linear responses (α polarizability) and the nonlinear responses (β hyperpolarizability) to a homogeneous electric field. The quantities (vector μ_0, tensor α and tensor β) are very important quantities for characterizing the molecule.

A neutral atom is placed in a static external electric field **F**. If the field is not too large, and the response (α polarizability) of the atom is isotropic , and induced dipole moment will be proportional to the electric field, and can be written

$$\hat{\mu} \; = \; \alpha \; \hat{F} \tag{2.15}$$

with α is the constant of proportionality — scalar quantity.

For a molecule with spherical symmetry, the polarizability is well-approximated by a single constant — scalar quantity, the polarizabilty is also isotropic. However, for many molecules being not spherical symmetry, the polarizability cannot be characterized by a single constant. For example, the charge distribution along the internuclear axis is longer than perpendicular to this axis for H_2 molecules, and thus it can be expected that the charge separation induced by external electric field is be greater along the internuclear axis than along a perpendicular axis[12]. In such case, a single scalar quantity is not sufficient to describe the polarizability. The most general way to transform one vector **F** to another μ is defined by a second-rank Cartesian tensor as in matrix form

$$\begin{pmatrix} \mu_x \\ \mu_y \\ \mu_z \end{pmatrix} = \begin{pmatrix} \alpha_{xx} & \alpha_{xy} & \alpha_{xz} \\ \alpha_{yx} & \alpha_{yy} & \alpha_{yz} \\ \alpha_{zx} & \alpha_{zy} & \alpha_{zz} \end{pmatrix} \begin{pmatrix} F_x \\ F_y \\ F_z \end{pmatrix} \tag{2.16}$$

For a static field, the polarizability tensor is symmetry.

2-1-2 Basic dielectric relations

In the vacuum, the electric field about a charge q at a distance r is defined by

$$F_v = \frac{q}{4\pi\varepsilon_0 r^2} \tag{2.17}$$

Now consider the electric field between two plates, the area of the plates is A, and each one has a surface charge density σ. If the medium between plates is a

vacuum, the electric field is derived as (atomic units), see Fig. 4(a)[13]

$$F_v = \frac{\sigma}{\varepsilon_0} \qquad (2.18)$$

But if there existing dielectric medium between two plates, the electric field will be reduced due to the polarization P of the material. The field distorts the atoms and molecules, and orients existing dipoles to create a field opposing the applied field. So the resultant field is reduced[13]. Now P called as polarization is defined as dipole moment per unit volume. Consider a plate of area A, length L. Its total dipole moment due to polarization is

$$P \times \text{volume} = PAL = PA \times L = \text{end charge} \times \text{length} \qquad (2.19)$$

Therefore, the effective charge density on the plates is ($\sigma - P$). The resultant field is in eq. (2.20) (see Fig. 4(b)[13])

$$F = \frac{\sigma}{\varepsilon} = \frac{\sigma - P}{\varepsilon_0} \qquad (2.20)$$

Rearrange eq. (2.20) and combine with eq. (2.18), the basic relation of polarization and electric field is obtained.

$$P = \sigma - F\varepsilon_0 = F(\varepsilon - \varepsilon_0) = F\varepsilon_0\left(\frac{\varepsilon}{\varepsilon_0} - 1\right) = F\varepsilon_0(\varepsilon_r - 1) = F\varepsilon_0\chi_e \qquad (2.21)$$

Electric susceptibility (χ_e) is defined through eq. (2.21), and is related to the relative permittivity (dielectric constant)

$$\chi_e = \varepsilon_r - 1 = \frac{P}{F\varepsilon_0} \qquad (2.22)$$
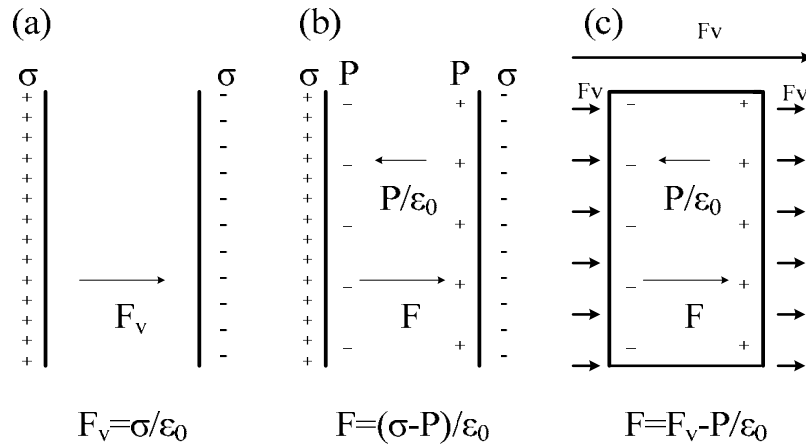
Fig. 4 (a)The field F_v between plates in vacuum.(b) The field in the dielectric medium is polarized, and it is reduced to F.(c) Relation between F and F_v

2-1-3 Lorentz local field and Clausius-Mossotti equation

Let us begin with considering all kinds of electric fields. F_0 is applied external field, and F_1 is the field of the surface induced charge density on the boundary, and it is due to the uniform polarization of the surface charge density. F_1 is also called depolarization field which is opposed to the applied field F_0 within the body. F is the addition of F_0 and F_1, and is called macroscopic electric field. (see Fig. 5[14]).
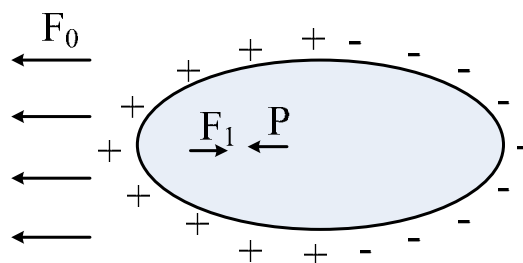
Fig. 5 The applied external field F_0. The depolarization field F_1 is opposite to P. And the macroscopic electric field F, $F=F_0+F_1$

Now an expression of local field F_{local} at a general lattice site is discussed. The local field that acts at the site of an atom is different from the macroscopic electric field F. If it is in a sphere, the macroscopic electric field can be seen in eq. (2.21) where the value of depolarization field is from depolarization factor of a sphere[14].

$$F = F_0 + F_1 = F_0 - \frac{1}{3\varepsilon_0}P \qquad (2.23)$$

The local field at an atom is the sum of the electric field F_0 from external sources and of the filed from the dipoles within the specimen. It is written as

$$F_{local} = F_0 + F_1 + F_2 + F_3 \qquad (2.24)$$

where F_0 = applied external field. F_1 = depolarization field, from a charge density of the outer surface. F_2 = Lorentz cavity field, from polarization charges inside of a spherical cavity cut out of the specimen with the reference atom as center. F_3 = field inside cavity. More details in Fig. 6[14]
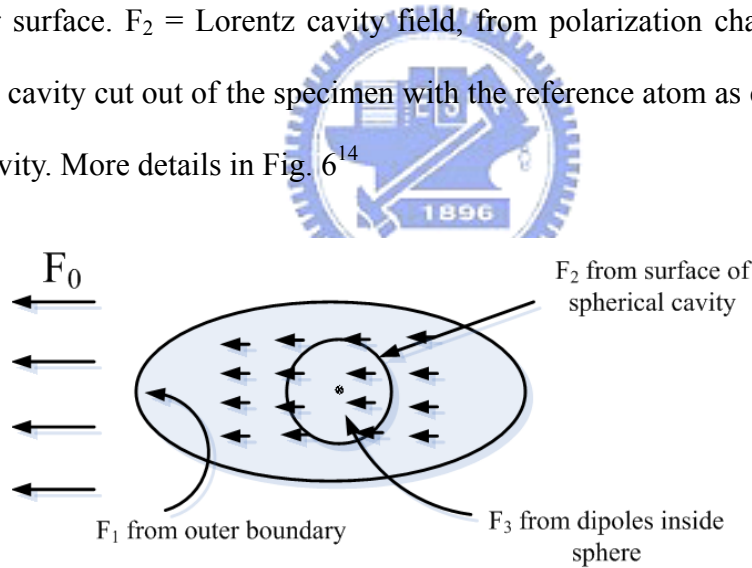
Fig. 6   The internal electric field at an atom in a crystal is the sum of the applied field F_0 and of the field due to the other atoms in the crystal. The standard method is summation of the dipole fields of the other atoms. First, it sums individually over a moderate number of neighboring atoms inside an imaginary sphere concentric with the reference atom: this is defined by the field F_3. The atoms outside the sphere can be contributed to the field at a reference point is $F_1 + F_2$.

If atomic arrangement is cubic symmetry in a crystal or the array of dipoles is random in a liquid or a glass, the inside field F_3 is zero. So the field F_3 depends on the crystal structure.

Now, let us start to discuss the Lorentz cavity field F_2. An annulus on the surface of a cavity is constructed. (see Fig. 7[13])
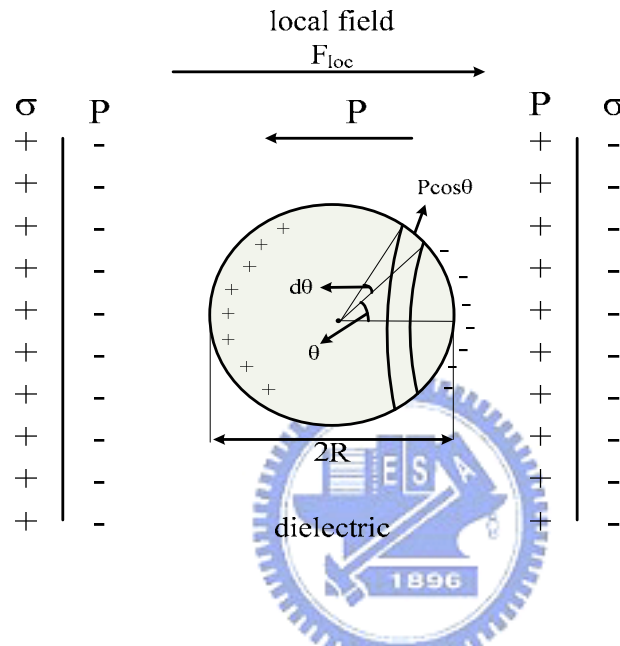
Fig. 7   charge distributions in a spherical cavity within a dielectric.

From Fig. 7, the charge on the annulus is

$$-P\cos\theta\ 2\pi R\sin\theta\ Rd\theta \tag{2.25}$$

At the center of the cavity it produces a coulomb field along the annulus. The vertical components cancel off, and the horizontal ones are additive from Fig. 4.

$$\left(\frac{1}{4\pi\varepsilon_0}\right)P\cos\theta\ 2\pi R\sin\theta Rd\theta\frac{1}{R^2}\cos\theta=\left(\frac{1}{2\varepsilon_0}\right)P\cos^2\theta\sin\theta d\theta \tag{2.26}$$

For the whole sphere, the net field F_2 is

$$F_2 = \frac{P}{2\varepsilon_0} \int_0^\pi \cos^2 \theta \sin \theta d\theta = \frac{P}{3\varepsilon_0} \qquad (2.27)$$

Finally, if atomic arrangement is cubic array or random ($F_3 = 0$) and the cavity is spherical, the local field is

$$F_{loc} = F_0 + F_1 + F_2 = F + \frac{P}{3\varepsilon_0} \qquad (2.28)$$

eq. (2.28) is the Lorentz relation.

The polarizability α of an atom is defined in term of the local electric field at the atom.

$$\mu = \alpha F_{loc} \qquad (2.29)$$

The polarization of a crystal can be expressed as the product of the polarizability of the atoms multiplied by the local electric field.

$$P = n\mu = n\alpha F_{loc} = n\alpha \left(F + \frac{P}{3\varepsilon_0} \right) \qquad (2.30)$$

where n called as number density is defined as total number of objects per unit volume, and the unit of P is dipole moment per unit volume.

Form eq. (2.30) basic relation between P and F in dielectric is obtained as

$$\frac{P}{F} = \frac{n\alpha}{1 - n\alpha/3\varepsilon_0} \qquad (2.31)$$

with which the dielectric constant in eq. (2.22) becomes

$$\chi_e = \varepsilon_r - 1 = \frac{P}{\varepsilon_0 F} = \frac{n\alpha}{\varepsilon_0 - n\alpha/3} \qquad (2.32)$$

and

$$\varepsilon_r + 2 = (\varepsilon_r - 1) + 3 = \frac{3\varepsilon_0}{\varepsilon_0 - n\alpha/3} \tag{2.33}$$

Finally, eq. (2.32) divided eq. (2.33) leads to

$$\frac{\varepsilon_r - 1}{\varepsilon_r + 2} = \frac{n\alpha}{3\varepsilon_0} \tag{2.34}$$

This formula is known as the Clausius-Mossotti equation.

Moreover, a practical form is obtained by replacing the number density by the mass density ρ.

$$n = \frac{N}{V} = \frac{N_A * \text{mol}}{V} = \frac{N_A(m/M)}{V} = \frac{N_A \rho}{M} \tag{2.35}$$

with N_A is the Avogadro constant, m is the mass of the sample and M is the Molar mass of the molecules.

Finally, the Clausius-Mossotti equation can be written as

$$\alpha = \frac{3\varepsilon_0 M}{N_A \rho} \left(\frac{\varepsilon_r - 1}{\varepsilon_r + 2} \right) \tag{2.36}$$

The polarizability which is one of atomic properties is related to many important bulk properties of a collection of particles including the dielectric constant ε_r, the electric susceptibility χ_e, the refractive index η, etc[12].

If there is the permanent electric dipole moment μ_0 in the molecule, the polarizability is related to the dielectric constant by the Debye equation.

$$\alpha + \frac{\mu_0^2}{3kT} = \frac{3\varepsilon_0 M}{N_A \rho} \left(\frac{\varepsilon_r - 1}{\varepsilon_r + 2} \right) \tag{2.37}$$

where μ_0 is the permanent dipole moment, k is Boltzmann's constant and T is the absolute temperature. (more details in 2-1-4 Polarizability)

The index of refraction is related to the polarizability by the Lorentz-Lorenz formula.

$$\alpha = \frac{3\varepsilon_0 M}{N_A \rho}\left(\frac{\eta^2 - 1}{\eta^2 + 2}\right) \qquad (2.38)$$

This formula is valid for non-polar molecules or at frequency high enough that the permanent dipole moments cannot follow the electric field. The Lorentz-Lorenz equation and Clausius-Mossotti equation are related by the Maxwell relation $\varepsilon_r = \eta^2$ [12].

2-1-4 Orientation and distortion polarization

As is seen from Fig. 4 (b), when a external field in the dielectric medium, the effective electric field between the plates must be reduced. The reduced field due to polarization of the medium is affected by two reasons. The first one is that the molecule of the medium has a permanent dipole moment, and this effect is known as orientation polarization. The orientation polarization is temperature dependent and its value decreases with an increase of temperature because the random thermal collisions oppose the tendency of the permanent dipole moments to orient themselves in the electric field [15]. This magnitude of the effect can be calculated from Boltzmann distribution. The energy of a dipole in a local field F_{local} along the z-axis is

$$E(\theta) = -\mu_z F_{loc} = -\mu F_{loc}\cos\theta, \text{ with } 0 \le \theta \le \pi \qquad (2.39)$$

The probability dp(θ) that a dipole has an orientation in the range θ to θ+dθ is

$$dp(\theta) = \frac{e^{-E(\theta)/kT} \sin\theta d\theta}{\int_0^\pi e^{-E(\theta)/kT} \sin\theta d\theta}$$

(2.40)

The average value of z component of the dipole moment is

$$\langle \mu_z \rangle = \int \mu \cos\theta dp = \mu \int \cos\theta dp = \mu \frac{\int_0^\pi e^{x\cos\theta} \cos\theta \sin\theta d\theta}{\int_0^\pi e^{x\cos\theta} \sin\theta d\theta}$$

$$, x = \frac{\mu F_{loc}}{kT}$$

(2.41)

Finally the average dipole moment along the z-axis is obtained.

$$\langle \mu_z \rangle = \mu L(x) \quad, L(x) = \frac{e^x + e^{-x}}{e^x - e^{-x}} - \frac{1}{x}$$

(2.42)

The function L(x) is called Langevin function.

When $\mu F_{loc} \ll kT$ corresponding to $x \ll 1$, the Langevin function is

$$L(x) \approx \frac{1}{3}x = \frac{\mu F_{loc}}{3kT}$$

(2.43)

From eq. (2.29) and (2.43), we will obtain

$$\alpha_o = \frac{\mu^2}{3kT}$$

(2.44)

Here α_o is called orientation polarizability, and the eq. (2.44) exists only at

$\mu F_{loc} \ll kT$.

The second version is that it always exists whether the molecule is polar or not. For the electrons to shift relative to the positive charges, and this is called as electronic polarization, while atoms are shifted relative to each other called as atomic polarization. If the position of a molecule is disturbed by a collision, a new dipole is immediately induced again in the direction of field. However, the

distortion polarization is independent on the temperature[15]. The sum of above two polarization effects is called distortion polarization.

2-1-5 A summary of polarization

The electric field gives rise to a dipole moment by the following effects[16]:

1. Translation (distortion) effects:

   The electrons are shifted relative to the positive charge (electronic polarization)

   Atoms or atom groups are displaced relative to each other (atomic polarization)

2. Rotation (orientation) effect:

   The electric field trends to direct the permanent dipole moments.
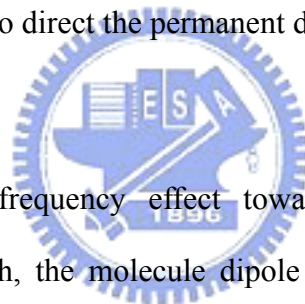
Now let us consider frequency effect toward polarizability. When the frequency of the field is high, the molecule dipole cannot change direction fast enough to follow the field. Therefore permanent dipole moment doesn't contribute to the polarization at microwave region, orientation polarizability is lost. For higher frequency, because the molecule is bent and stretched in the frequency of Infrared-Ray region by the applied field, the molecule dipole moments change accordingly. The time taken for a molecule to bend is approximately the inverse of the molecular vibrational frequency, so it will lose the contribution of the atomic polarization. At even higher frequency (about visible region), only the electrons are mobile enough to follow the rapidly changing direction of the field, so it only remains electronic polarizability[17]. (See Fig. 8)
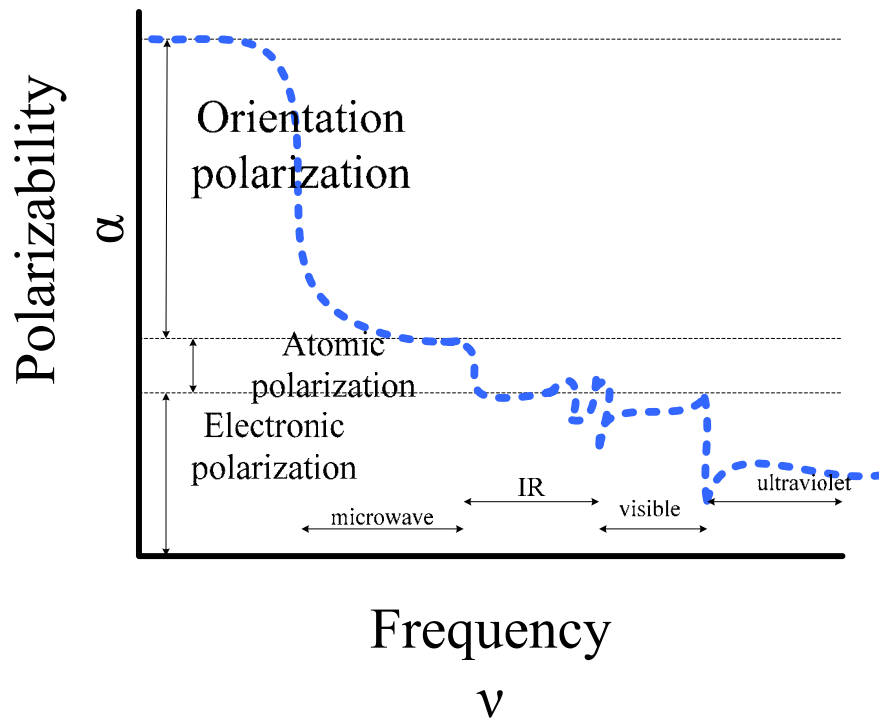
Fig. 8　The general form of the variation of the polarizability with the frequency.
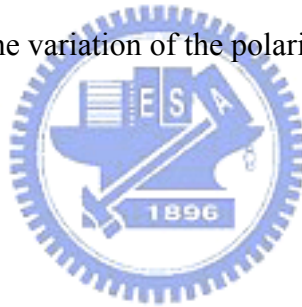
2-2 Charge population

2-2-1 Mullikan charge

Assuming the MO (φ) can be expanded in a set of basis functions (χ)

$$\phi_i = \sum_{\alpha}^{M\,basis} c_{\alpha i} \chi_\alpha \qquad (2.45)$$

The electron density (ρ) which is equal to the square of the MO (φ) can be written as

$$\rho_i = \phi_i^2 = \sum_{\alpha\beta}^{M\,basis} c_{\alpha i} c_{\beta i} \chi_\alpha \chi_\beta \qquad (2.46)$$

The total electrons (N_{elec}) are equal to integrating and summing over all occupied MOs.

$$N_{elec} = \sum_i^{N_{occ}} \int \phi_i^2 dr$$

$$= \sum_i^{N_{occ}} \sum_{\alpha\beta}^{M\,basis} c_{\alpha i} c_{\beta i} \int \chi_\alpha \chi_\beta dr = \sum_i^{N_{occ}} \sum_{\alpha\beta}^{M\,basis} c_{\alpha i} c_{\beta i} S_{\alpha\beta} \qquad (2.47)$$

The eq. (2.47) can be generalized by introducing an occupation number (n) for each MO, see eq. (2.48)

$$N_{elec} = \sum_i^{N_{occ}} n_i \int \phi_i^2 dr = \sum_{\alpha\beta}^{M\,basis} \left(\sum_i^{N_{occ}} n_i c_{\alpha i} c_{\beta i} \right) S_{\alpha\beta} = \sum_{\alpha\beta}^{M\,basis} D_{\alpha\beta} S_{\alpha\beta} \qquad (2.48)$$

The Mulliken population analysis uses the $\mathbf{D} \cdot \mathbf{S}$ matrix for separating the electron density into atomic contributions. A diagonal element $D_{\alpha\alpha}S_{\alpha\alpha}$ is the number of electrons on the α AO, and off-diagonal element $D_{\alpha\beta}S_{\alpha\beta}$ is the number of

electrons shared equally by α AO and β AO. The Mulliken electron population on atom A is defined as in eq. (2.49)

$$\rho_A = \sum_{\alpha \in A}^{M\ basis} \sum_{\beta=1}^{M\ basis} D_{\alpha\beta} S_{\alpha\beta} \qquad (2.49)$$

The Mulliken net charge on atom A is the sum of the nuclear and electronic contributions.

$$Q_A = Z_A - \rho_A \qquad (2.50)$$

However, Mulliken population analysis doesn't offer exact charges of the individual atom, it only provides the trend, because partition of the charge contribution is equal. Moreover, atomic charges calculated from the Mulliken analysis will not converge to a constant value when the size of the basis set is increasing. Larger basis set is usually involving the addition of more polarization basis functions or diffuse basis function, it will give rise to unpredicted change in the atomic charge. So Mulliken population analysis is affected largely by basis functions, and it usually is most useful for comparing trends in charge distributions, when small- or medium-size basis sets are used[10].

2-2-2 Atomic polar tensor charge

The atomic polar tensor V^{APT} of atom A is defined by the first derivatives of the dipole moment with respect to the nuclear coordinates[18] in eq. (2.52) and it can be used to determine intensities of IR absorptions due to the intensity is given by eq. (2.51).

$$IR \ \text{intensity} \ \propto \ \left(\frac{\partial \mu}{\partial R} \right)^2 \tag{2.51}$$

Here R is the nuclear coordinates.

$$V^{APT} = \begin{pmatrix} \dfrac{\partial \mu_x}{\partial x} & \dfrac{\partial \mu_x}{\partial y} & \dfrac{\partial \mu_x}{\partial z} \\[2mm] \dfrac{\partial \mu_y}{\partial x} & \dfrac{\partial \mu_y}{\partial y} & \dfrac{\partial \mu_y}{\partial z} \\[2mm] \dfrac{\partial \mu_z}{\partial x} & \dfrac{\partial \mu_z}{\partial y} & \dfrac{\partial \mu_z}{\partial z} \end{pmatrix} \tag{2.52}$$

The definition of atomic polar tensor charge on atom A is one-third of the trace over the APT[18], see eq. (2.53)

$$Q_A^{APT} = \frac{1}{3} \left(\frac{\partial \mu_x}{\partial x} + \frac{\partial \mu_y}{\partial y} + \frac{\partial \mu_z}{\partial z} \right) \tag{2.53}$$

Because dipole moment derivatives determine IR absorptions, APT charges are directly related to experimentally observable quantities[19]. Moreover, APT analysis has the following properties: (1) the atomic charges should be invariant with respect to rotations and translations of the molecule; (2) APT charges sum up to the total electric charges of the molecule; (3) APT charge isn't directly related to the choice of a particular basis set , its basis set dependent stems only from the fact that the basis set is not complete[18]. So the basis-set dependence is modest, although basis-set convergence isn't reported[20]. But APT charges are sensitive to the electron correlation in the wave function, it can be seen in Table 1[21]. A measure for the sensitivity of a particular change definition toward electron correlation is provided by the difference q (QCISD) – q (SCF). It is very obvious that APT charge exhibits the largest correlation effect and Mulliken population analysis appears to be relatively in sensitive to the electron correlation[21]. So the observation that APT

appears to be much less sensitive to the basis set than to electron correlation.

Table 1: Correlation contribution to different charge definitions at QCISD/cc-pVDZ level

| | | q(QCISD)-q(SCF) | | | |
		Mulliken	CHELPG	NPA	APT
BH	H	0.000	−0.068	0.018	−0.048
	B	0.000	0.068	−0.018	0.048
C_2H_2	H	−0.005	−0.031	−0.008	−0.021
	C	0.005	0.031	0.008	0.021
CH_4	H	0.005	−0.006	0.003	0.007
	C	−0.021	0.025	−0.011	−0.028
CO	C	−0.084	−0.055	−0.121	−0.151
	O	0.084	0.055	0.121	0.151
CO_2	O	0.087	0.085	0.109	0.202
	C	−0.173	−0.170	−0.217	−0.406
H_2CO	O	0.081	0.074	0.097	0.169
	C	−0.079	−0.051	−0.100	−0.127
	H	−0.001	−0.011	0.002	−0.021
H_2O	O	0.019	0.057	0.042	0.095
	H	−0.009	−0.028	−0.021	−0.048
H_2S	S	0.016	0.029	0.010	0.030
	H	−0.008	−0.015	−0.005	−0.015
HCl	H	−0.018	−0.017	−0.016	−0.037
	Cl	0.018	0.017	0.016	0.037
HCN	H	−0.016	−0.034	−0.010	−0.031
	C	−0.032	−0.002	−0.039	−0.068
	N	0.048	0.037	0.049	0.098
HF	H	−0.012	−0.028	−0.026	−0.053
	F	0.012	0.028	0.026	0.053
NH_3	N	0.021	0.079	0.039	0.096
	H	−0.007	−0.026	−0.013	−0.032
NNO	N	0.008	0.024	0.003	0.107
	N	−0.135	−0.123	−0.121	−0.345
	O	0.127	0.099	0.118	0.238
PH_3	P	−0.018	0.033	−0.032	−0.035
	H	0.006	−0.011	0.010	0.012
SO_2	S	−0.203	−0.122	−0.293	−0.405
	O	0.092	0.061	0.146	0.203

2-3　Dipole moment[16]

The dipole moment of a point charge q relative to a fixed point is defined as q**r**, in which **r** is the radius vector from the fixed point to e. Hence, the dipole moment of a system of charges qi, relative to a fixed origin is defined as:

$$\hat{\mu} = \sum_i q_i \hat{r}_i \tag{2.54}$$

If the net charge of the system is zero, the dipole moment is independent of the choice of the origin. The eq. (2.54) can be written in another way by introducing the positive and negative charges in eq. (2.55)

$$\hat{\mu} = \sum_{positive} q_i \hat{r}_i + \sum_{negative} q_i \hat{r}_i \tag{2.55}$$

For two atoms of a system (Fig. 9), the dipole moment can be written as

$$\hat{\mu} = q\hat{R}_+ + (-q)\hat{R}_- = q(\hat{R}_+ - \hat{R}_-) = q\hat{L} \tag{2.56}$$
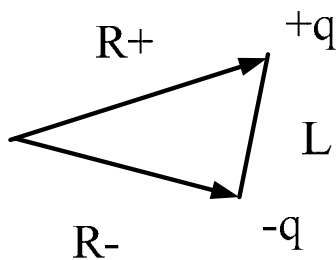
Fig. 9　The dipole moment in two atoms of a system

From eq. (2.56) it is very clear that we can choose one atom as the origin, and dipole moment will be equal to charge multiplied by bond length directly.

It is the same for three or more atoms of a system. For example, in three

atoms of a system, we choose the A atom as the origin for $(x_2, y_2) = (0,0)$, and dipole moment is as in Fig. 10.

$$\mu = q_1 \cdot \hat{r}_{12} + q_3 \cdot \hat{r}_{23} \qquad (2.57)$$

It is also written as

$$\mu_x = q_1 x_1 + q_3 x_3$$
$$\mu_y = q_1 y_1 + q_3 y_3$$

When the B atom is identical to the C atom, μ_x is equal to zero. And μ_y can be calculated from

$$\mu = \mu_y = 2qr \cos\frac{\alpha}{2} \qquad (2.58)$$

where $q = q_1 = q_3$ and $r = r_{12} = r_{23}$.
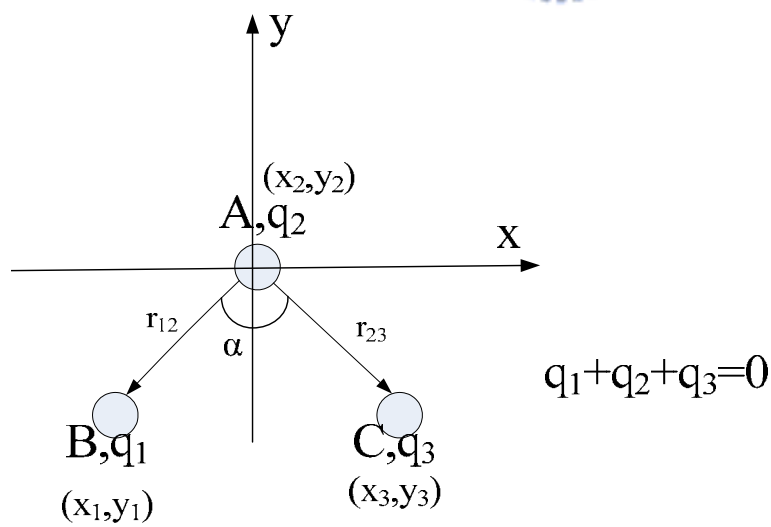
Fig. 10   The dipole moment in tree atoms of a system.

2-4 Density Functional Theory

2-4-1 Historical Background

Thomas (1926) and Fermi (1927) are the pioneering scientists to use the electron density rather than wave function for expressing approximate energy for the first time. They applied quantum statistical model (uniform electron gas) to the kinetic energy but treated the electron-nuclear and electron-electron interactions in classical way. The most important part is no exchange and correlation effect in this model. The Thomas-Fermi total energy is expressed in terms of density as[22].

$$E_{TF} = \frac{3}{10}\left(3\pi^2\right)^{\frac{2}{3}} \int \rho^{\frac{5}{3}}(\bar{r})d\bar{r} - Z\int \frac{\rho(\bar{r})}{r}d\bar{r} + \frac{1}{2}\iint \frac{\rho(\bar{r}_1)\rho(\bar{r}_2)}{r_{12}}d\bar{r}_1 d\bar{r}_2 \qquad (2.59)$$

Later on, Slater (1951) added the Hartree-Fock exchange term and exchange energy can be expressed approximately as

$$E_X[\rho] \cong C_X \int \rho(\bar{r})^{\frac{4}{3}}d\bar{r} \qquad (2.60)$$

To improve the quality of exchange energy, semiempirical parameter α was introduced to C_X. It is called Xα method in one of density functional approaches.

Hohenberg and Kohn (1964) brought up two theorems that make big contribution to the present DFT. The first one is that the ground state electronic density is uniquely specified by the given external potential V_{ext}, and it also means electron density ρ(r) defines all terms in the Hamilton operator[23]. In other words, the ground state electronic density and the ground state wave function can be used alternatively as full descriptions of the ground state of the system[11]. The second one is variational principle applied to density functionals. It could calculate ground state

energy by inserting approximate density, see eq. (2.61). E_0 represents the minimum value of the system.

$$E_0 \leq E[\tilde{\rho}] = T[\tilde{\rho}] + E_{Ne}[\tilde{\rho}] + E_{ee}[\tilde{\rho}] \tag{2.61}$$

Kohn and Sham (1964) considered a fictitious system of non-interacting particles, and in order to ensure that the system has the same density and energy as the real system, those particles are assumed moving in the external potential V_{eff} $(\mathbf{r})$[22]. In the other hand, the Kohn-Sham system of the electrons, that do not interact with each other at all (as if their charges are equal zero) but interact with the nuclei, they are subject to an external potential V_{eff} $(\mathbf{r})$[11], as described in the following[22].

$$E_e = T_0\left[\rho(\vec{r})\right] + \int V_{eff}(\vec{r})\rho(\vec{r})d\vec{r} \tag{2.62}$$

$$V_{eff}(\vec{r}) = \frac{\partial T}{\partial \rho} - \frac{\partial T_0}{\partial \rho} + V_{ext}(\vec{r}) + V_C(\vec{r}) + \frac{\partial E'_{xc}}{\partial \rho} \tag{2.63}$$

E'_{xc} is called as exchange correlation energy in which exchange part is from Hartree-Fock approximation, and correlation effect is obtained from extra correlation contributions (beyond the Hartree-Fock approximation). V_{ext} is the interaction of nuclei and electrons. V_c is the classical Coulomb operator, then there is a self-interaction of electron cloud with itself.

$$V_c = \sum_{j=1}^{N} \hat{J}_j(\hat{r}) \tag{2.64}$$

Now the exact form of effective potential V_{eff} is still unknown, so that the exchange-correlation potential V_{xc} is to be determined.

$$\frac{\partial T}{\partial \rho} - \frac{\partial T_0}{\partial \rho} + \frac{\partial E'_{xc}}{\partial \rho} \equiv \frac{\partial E_{xc}}{\partial \rho} \equiv V_{xc}(\vec{r}) \tag{2.65}$$

Finally, the total DFT energy of Kohn-Sham theorem can be written

$$
\begin{aligned}
&E_{DFT} = T_0\left[\rho\left(\bar{r}\right)\right] + \int\left[V_{ext}\left(\bar{r}\right) + V_C\left(\bar{r}\right) + Vxc\left(\bar{r}\right)\right]\rho\left(\bar{r}\right)d\bar{r} \\
&\Leftrightarrow E_{DFT}\left[\rho\right] = T_0\left[\rho\right] + E_{ne}\left[\rho\right] + J\left[\rho\right] + E_{XC}\left[\rho\right]
\end{aligned}
\tag{2.66}
$$

The most importance in eq. (2.66) is the exchange-correlation energy. A lot of approximations have been carried out for getting the accurate exchange-correlation energy. In the Local Density Approximation (LDA) it is assumed that uniform electron gas is in the system, in order to ensure that the electron density is constant in space, the exchange-correlation energy isn't related with variations of electron density. It means that we can calculate V_{xc} for the system as a function of the constant density. In the Generalized Gradient Approximation (GGA) it takes into account a non-uniform electron gas and includes electron density and the derivatives of the density in the expression of the exchange-correlation energy. On the other hand, E_{xc} depends not only on ρ at a given point (local), but also at the ρ nearby (non-local). Therefore, it is also called non-local approximations. If it includes higher derivatives of the density, it could be called meta-GGA approximation. At the beginning of the 1990s a new method was called Hybrid method combined the Hartree-Fock theory with Kohn-Sham theorem. Because the exchange energy is given exactly by Hartree-Fock theory and correlation energy is treated only by Kohn-Sham theorem, it will be more accurate to express the exchange-correlation energy. The most popular and famous method B3LYP functional is widely used in computation and it is defined in

$$
E_{xc}^{B3LYP} = \left(1\text{-}a\right)E_x^{LSDA} + aE_x^{HF} + b\Delta E_x^{B88} + \left(1-c\right)E_c^{LSDA} + cE_c^{LYP}
\tag{2.67}
$$

Three parameters a, b and c are determined by fitting to experimental data and

depend on the form of exchange and correlation energy. It is the classification of density functional below. (see Table 2)

Table 2:   Perdew classification of exchange-correlation functions[10]

Level	Name	Variables	Examples
1	Local density	ρ	L(S)DA , Xα
2	GGA	ρ , $\nabla\rho$	BLYP , OLYP , PW86 , PW91 , PBE
3	m-GGA	ρ , $\nabla\rho$,$\nabla^2\rho$ or more	B95 , VSXC , PKZB , TPSS
4	Hybid	ρ , $\nabla\rho$,$\nabla^2\rho$ or more and HF exchange	H+H , B3LYP , O3LYP , PBE0 , TPSSh
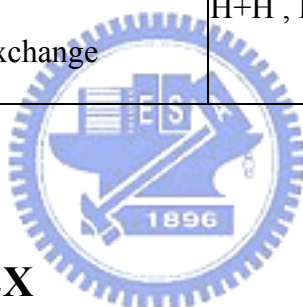
2-4-2 M05 and M05-2X

Now still there is one problem called as self-correlation error in some DFT methods. It stemmed from electron interacting with itself. Table 3 is about self-correlation error for one electron of Hydrogen atom. We can see the HF theory is free of self-correlation error for one-electron system, but other DFT methods clearly have self-correlation error.

Table 3:   Energy components [E_h] of various functionals for the hydrogen atom[23].

Functional	E_{tot}	$J[\rho]$	$E_X[\rho]$	$E_C[\rho]$	$J[\rho] + E_{XC}[\rho]$
SVWN	−0.49639	0.29975	−0.25753	−0.03945	0.00277
BLYP	−0.49789	0.30747	−0.30607	0.0	0.00140
B3LYP	−0.50243	0.30845	−0.30370[a]	−0.00756	−0.00281
BP86	−0.50030	0.30653	−0.30479	−0.00248	−0.00074
BPW91	−0.50422	0.30890	−0.30719	−0.00631	−0.00460
HF	−0.49999	0.31250	−0.31250	0.0	0.0

[a] Includes 0.06169 E_h from exact exchange.

M05[24] (for Minnesota 2005) and M05-2X[25] (for Minnesota 2005 with double the amount of nonlocal exchange) are the newly developed functionals. They both can be called hybrid methods, because they incorporate electron spin density, density gradient, kinetic energy density and Hartree-Fock exchange energy. The two new functionals have three advantages; one is incorporating kinetic energy density in a balanced way in the exchange and correlation functionals, the other is to satisfy the uniform electron gas limit, the third is free of self-correlation[25]. The M05 functional was parametrized by including both metals and nonmetals and is broadly applicable to organometallic, inorganometallic and nonmetallic bonding, thermochemistry, thermochemical kinetics, and noncovalent interaction[24]. So M05 performs well not only for main-group thermochemistry and radical reaction barrier but also for transition-metal to transition-metal interaction. The M05-2X functional was parametrized only for nonmetals and performed well for thermochemical kinetics and noncovalent interactions (weak interaction like hydrogen bond …etc), excluding metals[25].

2-5 Thermoeletric Phenomena

2-5-1 Historical Background

In 1822, Thomas Johann Seebeck published a paper describing that a compass needle was deflected when it was placed in a closed loop of two dissimilar metals that had one junction heated*. That was the first observation of the phenomenon of thermoelectricity. But he tried to relate this phenomenon to the earth's magnetic field. Of course, it didn't work because the phenomenon wasn't from the magnetic effect at all. Although Seebeck didn't understand it at that time, that effect was known as the Seebeck effect. Later in 1835, Jean Charles Athanase Peltier discovered that the temperature of a junction between two dissimilar metals changes when current flows between them[26]. At that time, it was not realized that this was related to the Seebeck effect. In 1838, Lenz discovered that heat is liberated or absorbed depending on the direction of the current flow across a junction of two dissimilar conductors[26]. That is the so–called Peltier effect is the absorption or generation of heat at a junction between two materials when current is flowing through them[26]. In 1851, William Thomson established a relationship between the Seebeck and Peltier coefficients, and predicted a third thermoelectric effect[26]. This effect is known as Thomson effect, which occurs when currents are flowing through a material placed in a temperature gradient[26]. Thomson can observe this effect experimentally corresponding to his predictions.

An electron in solids is an elementary particle, and can carry electric current. Because immense magnitudes of electrons are at thermal equilibrium in solids, they also carry heat and entropy[1]. In the presence of temperature gradient, electrons can

flow from a hot side to a cold side to cause the electric current. It is obvious that a coupling between thermal and electric phenomena, and is called as the thermoelectric effect.

2-5 -2 Seebeck effect

When two dissimilar materials are jointed together and the junctions are held at different temperatures (T and T+ΔT), a voltage different (ΔV) would be induced. The ratio of the voltage difference (ΔV) to temperature gradient (ΔT) is related to an intrinsic property of the materials called the Seebeck coefficient (S_e). Seebeck coefficient is very low for metals (only a few μV / K) and much larger for semiconductors (a few hundred μV / K)[27]. Using Seebeck effect, thermal energy can be converted to electric energy. When left side of the sample is heated in Fig. 11[1], the thermoelectric voltage is induced in proportion to the temperature difference[1]. If a bulb is connected to the sample, the electric energy is consumed at the bulb. Therefore, the thermoelectric materials can be used as a kind of battery[1].
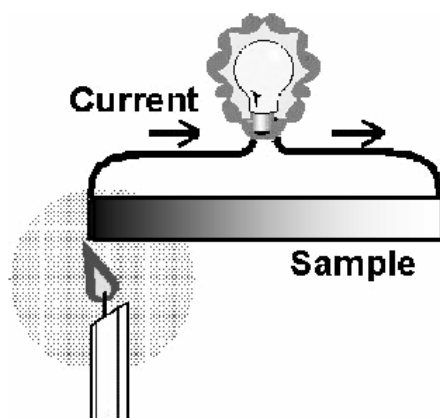
Fig. 11   Scheme of thermoelectric power generation.

In Fig. 6[28], two dissimilar conductors, A and B, have junctions at X and Y. If a temperature gradient exists between X and Y, a voltage difference (V) appears between two B segments. Under the open circuit condition, the Seebeck coefficient is defined as

$$S_e = \frac{dV}{dT} \qquad (2.68)$$
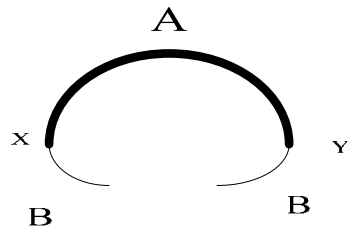
Fig. 12. The basic thermoelectric circuit.

In general, the energy conversion efficiency can be expressed as a function of the temperature and the so-called 'goodness factor' or thermoelectric figure-of-merit of the material (Z) is defined as.

$$Z\,T = \frac{S_e^{\,2}\,\sigma}{\kappa}\,T \qquad (2.69)$$

where S_e is Seebeck coefficient, σ is the electrical conductivity, κ is the total thermal conductivity ($\kappa_{phonon} + \kappa_{electron}$).

The electric power factor ($S_e^2 \sigma T$) is typically optimized in narrow-gap semiconductors as a function of carrier concentration ($\sim 10^{19}$ carriers / cm^3)[27]. If through doping, it will give the larger ZT. High-mobility carriers are most desirable, in order to have the higher electrical conductivity. However, the electronic conductivity increases with carrier concentration, but Seebeck coefficient decreases with carrier concentration in Fig. 13[1]. $\underline{S^2 / \rho}$ equal to $\underline{S^2 \sigma}$ is the electric power

factor. This factor goes to a maximum at an optimal carrier concentration n_o, below which the conductivity is too low, and above which the Seebeck coefficient is too small in Fig. 13[1].
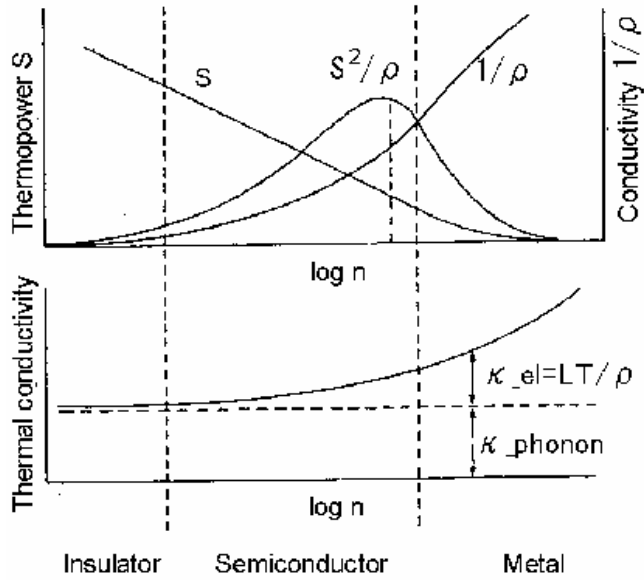
Fig. 13   Thermoelectric parameters as a function of temperature.

for Fig. 11 the efficiency of the power generator is given by[27]:

$$\eta = \frac{\text{energy consumed for a bulb}}{\text{heat energy absorbed at the hot side}}$$

$$= \frac{T_H - T_C}{T_H} \left[\frac{\sqrt{(1+ZT_M)} - 1}{\sqrt{(1+ZT_M)} + \left(\frac{T_C}{T_H}\right)} \right] \tag{2.70}$$

where T_H is hot-side temperature, T_C is cold-side temperature, T_M is the average temperature.

If ZT goes into infinity in eq. (2.70), the efficiency would approach the Carnot efficient limit that is equal to $(T_H - T_C) / T_H$.

The energy conversion efficiency as a function of the temperature difference and the figure-of-merit of different materials is Fig. 14[29]. It is very clear that an increase in temperature differences gives a increase in the heat conversion[29].
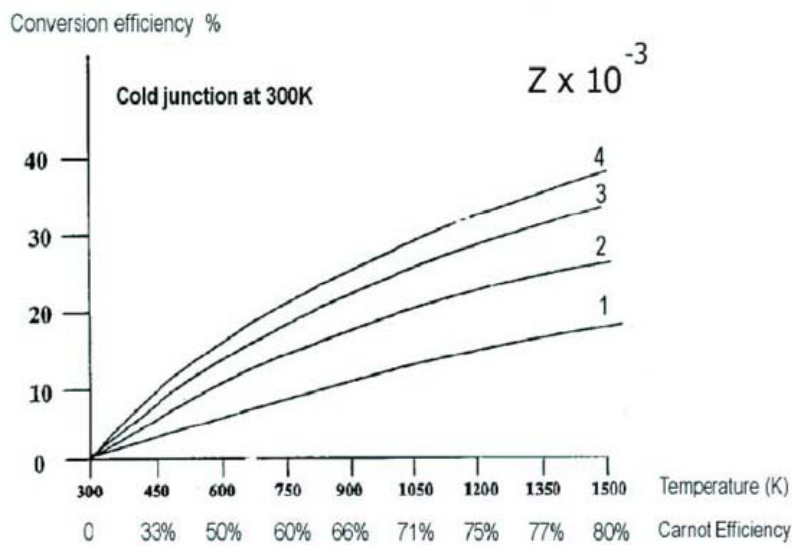
Fig. 14　Carnot efficiency and corresponding efficiency as the function of temperature and figure-of-merit (Z).

Chapter 3 Calculation

3-1 Determination of the structure

The electronic configuration of the Mg atom is [Ne] $3s^2$. From $3s^2$, we know the ground electronic configuration is ^1S, while the electronic configuration of the Si atom is [Ne] $3s^2 3p^2$, we also obtain the ground electronic configuration of Si is ^3P. The Mg_2Si molecule composed of $^1S + ^1S + ^3P$ might have 1-, 3- or 5-multiple states[30].

The electronic configuration of the Fe atom is [Ar] $4s^2 3d^6$. From $3d^6$, we know the ground electronic configuration of Fe is ^5D. The following, the electronic configuration of the Si atom is [Ne] $3s^2 3p^2$, we also obtain the ground electronic configuration of Si is ^3P. The $FeSi_2$ molecule composed of $^5D + ^3P + ^3P$ might have 1-, 3-, 5-, 7- or 9-multiple states[30].

The Gaussian 03 program is used to calculate the minimum energy in order to find out the ground state of Mg_2Si and $FeSi_2$ molecules respectively. Since transition metal and its' respective open-shell compounds usually have several low-lying states that are close to each other[31]. Therefore, when we optimize the $FeSi_2$ molecule, we don't know whether the obtained structure with minimum energy is correct or not. In order to ensure it is a global minimum, we use "stable=opt" keyword in Gaussian input file. This keyword is used to test and adjust the stability of wave function.

Here, B3LYP and CCSD levels are applied to optimize the Mg_2Si molecule with the basis set of 6-311G. According to the accurate calculations, the ground state

of Mg$_2$Si molecule is 3-multiple state with the parallel spin of 2 electrons (see Table 4 and Table 5), and the optimized structure of Mg2Si is C$_{2v}$ symmetry (see Fig. 15).

Table 4: B3LYP/6-311G for optimum results of Mg$_2$Si molecule. R (Si-1Mg) is the distance between the Si atom and the first Mg atom and its' unit is Angstrom. A(1Mg-Si-2Mg) is the angle ($\angle$1Mg,Si,2Mg).

B3LYP/6-311G					
multiplicity	energy	Frequency	R(Si-1Mg)	R(Si-2Mg)	A(1Mg-Si-2Mg)
1	-689.618387	134.7702	2.53192236	2.53192236	78.34844144
3	*-689.6270395*	99.926	2.6781793	2.6781793	72.94756733
5	-689.5836993	69.6101	2.94764684	2.94764684	59.7243576

Table 5: CCSD/6-311G for optimum results of Mg$_2$Si molecule.

CCSD/6-311G					
multiplicity	energy	Frequency	R(Fe-1Si)	R(Fe-2Si)	A(1Si-Fe-2Si)
1	-688.1614055	131.8995	2.59287117	2.59287117	78.1343544
3	*-688.1716205*	83.4749	2.76324017	2.76324017	75.26280165
5	-688.15725	29.2628	2.61830706	2.61830708	179.0189632
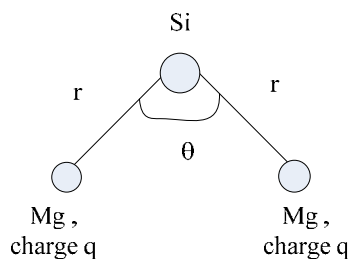
Fig. 15   Optimized structure of Mg_2Si

Here, we apply B3LYP and CCSD methods and the Pople style basis set (6-311G) and effective core potential (LANL2DZ) to optimize all structures. According to the accurate calculations, the ground state of $FeSi_2$ molecule is 5-multiple state with the parallel spin of 4 electrons (see Table 6, 7, 8 and 9), and optimized structure of $FeSi_2$ is C_{2v} symmetry (see Fig. 16).
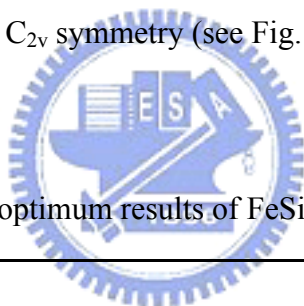
Table 6:   B3LYP/6-311G for optimum results of $FeSi_2$ molecule.

B3LYP/6-311G					
multiplicity	energy	Frequency	R(Fe-1Si)	R(Fe-2Si)	A(1Si-Fe-2Si)
1	-1842.357879	279.5418	2.142721	2.142721	67.34959956
3	-1842.417107	267.2064	2.2837303	2.2837303	61.49664695
5	*-1842.433828*	193.9053	2.3514793	2.3514793	58.961721
7	-1842.390517	59.8337	2.64606	2.91649	46.09917
9	-1842.331071	113.8058	2.6500867	2.6500867	70.62778204

Table7:   B3LYP/LANL2DZ for optimum results of FeSi$_2$ molecule.

B3LYP/LANL2DZ					
multiplicity	energy	Frequency	R(Fe-1Si)	R(Fe-2Si)	A(1Si-Fe-2Si)
1	-131.0389824	273.1597	2.1799708	2.1799717	65.03016334
3	-131.0907101	235.5565	2.3692525	2.3692523	60.51349789
5	***-131.0964158***	232.3818	2.3952707	2.3952707	57.35626941
7	-131.0379262	176.4525	2.4838927	2.4838927	58.2822207
9	-130.9867085	120.4974	2.4471927	2.4471927	81.15815227

Table 8:   CCSD/6-311G for optimum results of FeSi$_2$ molecule.

CCSD/6-311G					
multiplicity	energy	Frequency	R(Fe-1Si)	R(Fe-2Si)	A(1Si-Fe-2Si)
1	-1840.239849	237.8881	2.15013	2.15013	73.94434
3	-1840.27555	212.2495	2.40335	2.40335	63.86867
5	***-1840.295423***	207.4955	2.47692	2.47692	55.895
7	-1840.1896181	101.6277	2.270505	2.2705135	180.00000
9	-1840.2157592	60.7004	2.56777	2.73008	180.00000

Table 9:   CCSD/LANL2DZ for optimum results of $FeSi_2$ molecule.

CCSD/lanl2dz					
multiplicity	energy	Frequency	R(Fe-1Si)	R(Fe-2Si)	A(1Si-Fe-2Si)
1	-130.1843289	205.3564	2.20301	2.20301	70.79336
3	-130.2126973	232.8149	2.38794	2.38794	62.46974
5	*-130.2329031*	234.5013	2.42909	2.42909	56.28117
7	-130.1517204	65.8466	2.279	2.27899	175.29658
9	-130.144619	53.2995	2.640	2.64004	179.93606

Fe

r   r

θ

Si ,   Si ,
charge q   charge q
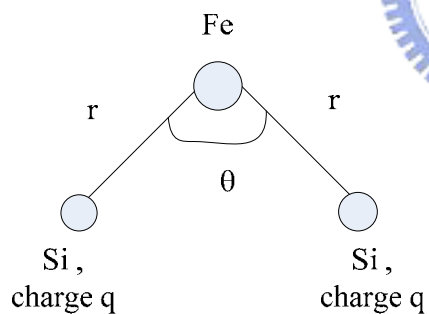
Fig. 16   Optimized structure of $FeSi_2$

3-2 Calculation of dielectric constant

From section 3-1, the ground state electronic configurations of Mg_2Si and $FeSi_2$ are proved to be 3-multiple and 5-multiple states, respectively. Then more precise methods and basis sets are applied to calculate. The all calculations of Mg_2Si are based on B3LYP, BLYP, M05 and M052X levels by the Pople style basis sets [6-311G, 6-311G(d), 6-311+G, 6-311+G(d)…etc] and effective core potential [LANL2DZ, CEP-31G and CEP-121G]. And for $FeSi_2$, the levels and basis sets used in calculations are the same as for Mg_2Si.

First of all, optimized structure is taken to calculate dipole moment, Helmholtz free energy, Mulliken charge and APT charge with electric field variant. Following the paper, the applied electric fields are 0.00, 0.01, 0.02, 0.03, 0.04, 0.05 and 0.06 atomic unit originally[9]. Finally, it shows that electric fields can be only applied from -0.01 to 0.01 a.u. in order to obtain the meaningful resulr. Energy, dipole moment, Mulliken charge and APT charge are fitted with electric field, and then the quadratic equations are obtained. The polarizability is obtained from the derivative of the quadratic equation. Finally, dielectric constant could be obtained from Clausis-Mossotti equation.

3-3 Calculation of Seebeck coefficient

The optimized Mg_2Si molecule is applied to calculate Helmholtz free energy with temperature variant. The range of temperature is varying from 300K to 800K[9]. The optimized $FeSi_2$ molecule is applied to calculate Helmholtz free energy with temperature variant. The range of temperature is varying from 300K to 900K.The obtained Helmholtz free energy above is converted to electron volt through unit conversion, due to the focus of being at unit charge now[9]. So the volts are fitted with temperature, and the quadratic equation is got directly. By the derivatives of quadratic equation with respect to temperature and combination with obtained dielectric constants previously[9], Seebeck coefficient is obtained.

Chapter 4 Result and Discussion

4-1 Magnesium Silicide (Mg_2Si)

4-1-1 Paper work

Following the procedures in Ref. 9 for Mg_2Si in which B3LYP method and 6-311G basis set are used. We have now added the other another three basis sets (6-311G (d), 6-311+G and 6-311+G (d)) in comparison with 6-311G, respectively. The total electronic energy is obtained at various electric fields: 0.00, 0.01, 0.02, 0.03, 0.04, 0.05 and 0.06 atomic unit (a.u.). Then energies are fit with respect to electric fields for each method and each basis set. (See Table 10)
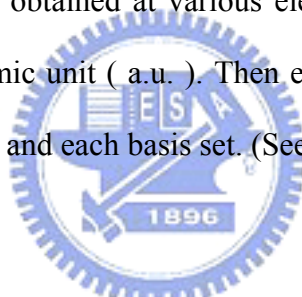
Table 10: Energies (E) are fit with electric fields (F) and polarizability volumes are obtained from deriving the fitting equations at the B3LYP level.

Mg_2Si (B3LYP)	Fitting equation	α_{tot} (Hartree/a.u.^{2})	α_{tot}(cm3)
6-311G	$E = -88.245F^2 - 1.1318F - 689.63$	177.6218	2.63E-23
6-311G(d)	$E = -87.955F^2 - 1.0027F - 689.64$	176.9127	2.62E-23
6-311+G	$E = -177.52F^2 + 0.2477F - 689.63$	354.7923	5.26E-23
6-311+G(d)	$E = -176.01F^2 + 0.2143F - 689.64$	351.8057	5.21E-23

Firstly, the fitting equation ($E = -88.245F^2 - 1.1318F - 689.63$) is taken as an illustration in the Table 10, due to the definition of dipole moment $\mu = -\left(\dfrac{\partial E}{\partial F}\right)$, the equation can be written as $\mu = 176.49F + 1.1318$. When F=1 (a.u.), μ=177.6218 (Hartree/a.u.). Then the polarizability α is assumed as being in the unit electric field, $\alpha = 177.6218$ (Hartree/a.u.^{2}). Finally we must convert unit (Hartree/a.u.^{2}) of the polarizability to polarizability volume (cm^3), See Table 10. Because the polarizability is from total energy, the polarizability volume is called total polarizability volume (α_{tot}).

Secondly, dipole moments are obtained at various electric fields (0 ~0.06 a.u.), and are fitted with fields, see Table 11. Because of $\alpha = \dfrac{\partial \mu}{\partial F}$ and the base of a unit electric field, distortion polarizability (α_d) is obtained easily.
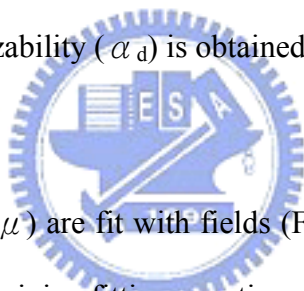
Table 11: Dipole moments (μ) are fit with fields (F) and distortion polarizability volumes are obtained from deriving fitting equations at the B3LYP level.

Mg$_2$Si(B3LYP)	Fitting equation	α_d (debye/a.u.)	α_d (cm3)
6-311G	$\mu = -102.46F^2 + 453.33F + 2.8494$	248.41	1.45E-23
6-311G(d)	$\mu = 15.238F^2 + 445.17F + 2.5882$	475.646	2.77E-23
6-311+G	$\mu = 1887.5F^2 + 758.3F + 1.5688$	4533.3	2.64E-22
6-311+G(d)	$\mu = 1371.2F^2 + 782.54F + 1.28$	3524.94	2.06E-22

4-1-2 Correction for electric field and polarizability

From Table 11, it can be clearly seen that the distortion polarizability is sensitive to the choice of the basis sets. In order to find out why distortion polarizability is so sensitive to the basis sets, we compare total electronic energy at a varying field with ionization energy from a minus of electronic HOMO energy without electric field in Table 12.

Table 12:   In B3LYP/6-311+G (d), total electronic energy with a varying electric field and the absolute value of the energy difference between electric fields: one exists the field and the other dose not. It also shows the HOMO, LUMO energy and ionization energy without electric field.

B3LYP/6-311+G(d)							
electric field (z-axis, a.u.)	-0.06	-0.05	-0.04	-0.03	-0.02	-0.01	0
E_e	-690.2525	-690.0270	-689.8504	-689.7385	-689.6616	-689.6376	-689.6385
$\mid E_e - E_e(F=0) \mid$	0.6140	0.3885	**0.2118**	0.1000	0.0230	0.0009	0.0000
HOMO							-0.1537
LUMO							-0.0982
ionization energy							**0.1537**

B3LYP/6-311+G(d)						
electric field (z-axis, a.u.)	0.01	0.02	0.03	0.04	0.05	0.06
E_e	-689.6586	-689.7014	-689.7887	-689.9164	-690.0692	-690.2588
$\mid E_e - E_e(F=0) \mid$	0.0200	0.0629	0.1502	**0.2778**	0.4306	0.6203
HOMO						
LUMO						
ionization energy						

In Table 12, it shows that when the electric field is outside [-0.04, 0.04] a.u., the absolute value of energy difference between electric fields: one exists the field and the other does not is larger than ionization energy (0.1537 hartree). It also means that the field strength outside of [-0.04, 0.04] a.u. is too large, and then leads the electrons to ionize and electronic structure is changed severely. But in the present work, we focus on the variation of energy and dipole moment in the smaller electric field. So we must choose smaller electric fields. Moreover, we make a plot of dipole moments against fields from -0.06 to 0.06 a.u. in Fig.15 with four basis sets.
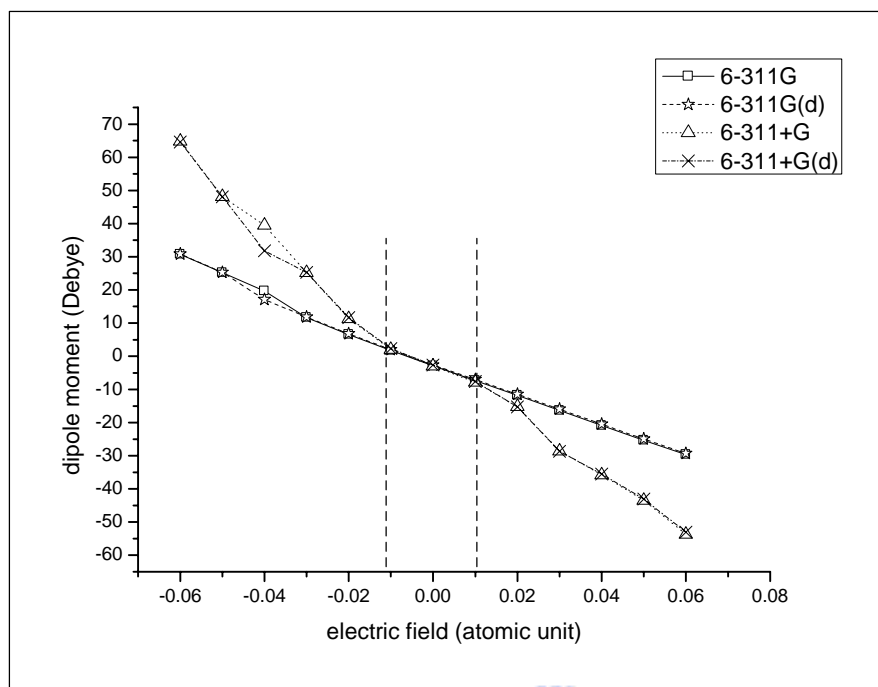
Fig. 17   Fitting plot of dipole moment versus electric field by four basis sets in

B3LYP level
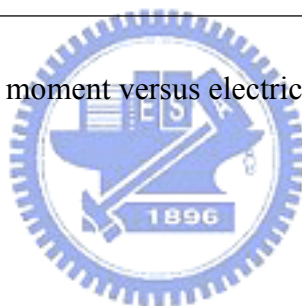
In Fig. 17, all four fitting lines coincide when electric field is in between -0.01

and 0.01 a.u. and are dispersive when field is outside of [-0.01, 0.01] a.u.. This is

due to effect of the stronger field, and results in obtaining dispersive fitting lines

and different distortion polarizability by four basis sets in Table 11. When the field

strength is larger, the convergence of the computation is out of control by the

perturbation method, and also the molecule is going to undergo multiple ionizations

at that strong field. Energy calculation is meaningless at $|F| > 0.01$ a.u.. On the other

hand, we want to obtain the convergent polarizability with different basis sets, so

the range of the field from -0.01 to 0.01 a.u. is chosen in the following

investigations. The results of the renewed fitting are listed in Table 13.

Table 13: Dipole moments (μ) are fit with electric field (F) and distortion polarizability volume. Fitting field is from -0.01 to 0.01 a.u..

Mg$_2$Si (B3LYP)	Fitting equation	α_d (debye/a.u.)	α_d(cm3)
6-311G	$\mu = 595.77F^2 - 454.13F - 2.8765$	737.41	4.30E-23
6-311G(d)	$\mu = 628.68F^2 - 449.92F - 2.6034$	807.44	4.71E-23
6-311+G	$\mu = 456.99F^2 - 489.37F - 2.9321$	424.61	2.48E-23
6-311+G(d)	$\mu = 454.91F^2 - 491.02F - 2.6724$	418.8	2.44E-23

In Table 13, it is quite obvious that distortion polarizability volume is still sensitive for using different basis set, especially for additional diffuse functions. In order to decrease the inconsistency in polarizability, we check that previously mentioned about the base of one a.u. of the electric field again. It is found that total energy from the Taylor expansion at F = 0 is more reasonable than at F=1 following the published paper to evaluate. (See eq. (4.1) and (4.2))

$$E(F)=E(0)+\left.\frac{\partial E}{\partial F}\right|_{F=0}F+\frac{1}{2}\left.\frac{\partial^2 E}{\partial F^2}\right|_{F=0}F^2+\frac{1}{6}\left.\frac{\partial^3 E}{\partial F^3}\right|_{F=0}F^3... \qquad (4.1)$$

$$-\left.\frac{\partial^2 E}{\partial F^2}\right|_{F=0} = \alpha \qquad (4.2)$$

Dipole moment is the same as total energy from the Taylor expansion. It can be written as

$$\mu = \mu_0 + \left.\frac{\partial \mu}{\partial F}\right|_{F=0} F + \frac{1}{2}\left.\frac{\partial^2 \mu}{\partial F^2}\right|_{F=0} F^2 + \frac{1}{6}\left.\frac{\partial^3 \mu}{\partial F^3}\right|_{F=0} F^3 + ... \qquad (4.3)$$

$$\boxed{\left.\frac{\partial \mu}{\partial F}\right|_{F=0} = \alpha} \qquad (4.4)$$

Now, total polarizability from the fitting of total energy and electric field and distortion polarizability from the fitting of dipole moment and field are evaluated in Table 14 and 15 again.
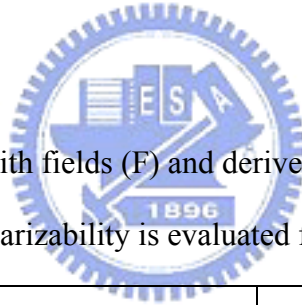
Table 14: Energy (E) is fit with fields (F) and derives polarizability. Fitting field is from -0.01 to 0.01 a.u. and polarizability is evaluated from Taylor expansion at F=0.

Mg$_2$Si (B3LYP)	Fitting equation	α_{tot} (Hartree/a.u.^{2})	α_{tot}(cm3)
6-311G	E = -89.259F^2 - 1.1259F - 689.63	178.518	2.65E-23
6-311G(d)	E = -88.426F^2 - 1.0182F - 689.64	176.852	2.62E-23
6-311+G	E = -95.367F^2 - 1.1492F - 689.63	190.734	2.83E-23
6-311+G(d)	E = -95.613F^2 - 1.047F - 689.64	191.226	2.83E-23

Table 15: Dipole moments (μ) are fit with fields and derive distortion polarizability. Fitting field is from -0.01 to 0.01 a.u. and polarizability is evaluated from Taylor expansion at F=0.

Mg$_2$Si (B3LYP)	Fitting equation	α_d(debye/a.u.)	α_d(cm3)
6-311G	$\mu = 595.77F^2 - 454.13F - 2.8765$	454.13	2.65E-23
6-311G(d)	$\mu = 628.68F^2 - 449.92F - 2.6034$	449.92	2.62E-23
6-311+G	$\mu = 456.99F^2 - 489.37F - 2.9321$	489.37	2.85E-23
6-311+G(d)	$\mu = 454.91F^2 - 491.02F - 2.6724$	491.02	2.86E-23

The total polarizability α_{tot} is the sum of the distortion polarizability α_d and orientation polarizability α_o, but by comparing Table 14 with Table 15 it shows that the polarizabilities from the fitting of energy or dipole moment is the same. Fitting results of dipole moment cannot be taken as distortion polarizability directly, because dipole moment in the calculation is derived from the quantum mechanical dipole operator.

$$\hat{\mu} = -\sum_i r_i + \sum_A Z_A R_A \qquad (4.5)$$

r$_i$ and R$_A$ are the vectors of the electrons and nucleus respectively, Z$_A$ represents nuclear charges.

The mean value of dipole moment is evaluated in eq. (4.6) directly.

$$\begin{aligned} \mu &= \left\langle \Psi_0 \left| -\sum_i r_i + \sum_A R_A Z_A \right| \Psi_0 \right\rangle \\ &= \left\langle \Psi_0 \left| -\sum_i r_i \right| \Psi_0 \right\rangle + \left\langle \Psi_0 \left| \sum_A R_A Z_A \right| \Psi_0 \right\rangle \\ &= \mu_{ele} + \mu_{nucl} \end{aligned} \qquad (4.6)$$

It shows clearly that the dipole moment as the function of electric field should represent total dipole moment including electron part and nucleus part. From Table 14 and 15 we can see that polarizability from the fitting results of the dipole moment and the electric field should be assumed as total polarizability, is the same as the result of the fitting from the total energy and the electric field.

4-1-3 Dielectric constant for solid Mg_2Si

For solid Mg_2Si, there are no translational and rotational motions in degrees of the freedom, so orientation polarizability has no contribution to total polarizability ($\alpha_o = 0$). Now, we must remove orientation polarizability from total polarizability. Because of the effect from Boltzmann distribution, the orientation polarizability can be written as

$$\alpha_o = \frac{\mu^2}{3kT} \qquad (4.7)$$

But it should be at $\mu F_{loc} \ll kT$ in eq. (4.7).

Applied electric field is 0.01 a.u. and temperature is 300K in our case. When B3LYP, with 6-311G basis set are used, the permanent dipole moment is 2.8765 Debye. But μF_{loc} (= 4.93E-20 J) is greater than kT (= 4.14E-21 J) in fact, so Boltzmann distribution isn't used in obtaining distortion polarizability.

We would like to understand is how to calculate the distortion polarizability directly. Because distortion polarizability is the sum of the electronic polarizability

and atomic polarizability, we can obtain electronic part from charge population directly. Moreover, for atomic polarizability, because it is about 5 % ∼ 10 % of the electronic polarizability, it can be almost neglected.

Starting from charge population, we adopt the Mulliken partial charge and APT partial charge to derive the Mulliken and APT dipole moment. Firstly, there is an optimized structure of Mg2Si at F = 0 in Fig. 18.
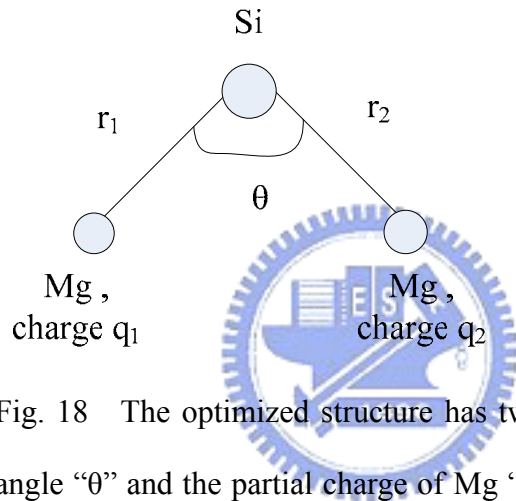
Fig. 18   The optimized structure has two bond length "r_1" and "r_2", angle "θ" and the partial charge of Mg "q_1" and "q_2". Here are $r_1 = r_2$ = r and $q_1 = q_2 = q$.

From Fig. 18 the dipole moment is derived in eq. (4.8)

$$\mu = \sum_i q_i r_i = q_1 \vec{r_1} + q_2 \vec{r_2} = q(\vec{r_1} + \vec{r_2}) = q\left(2r\cos\frac{\theta}{2}\right) \qquad (4.8)$$

Here r_1, r_2 and θ is calculated at electric field equal to zero and q is APT charge or Mulliken charge calculated with varying electric field. Because when perturbation of electric field is added, the output of the Mg$_2$Si geometry from G03 calculation isn't changed, only partial charges are changed. Therefore, we think that

the APT dipole and Mulliken dipole is only from electronic part. So we call the polarizability from APT and Mulliken dipole as electronic polarizability.

Mulliken and APT charge are chosen respectively and we can obtain two kinds of dipole moment, Mulliken dipole and APT dipole. Now, we compare all dipoles : dipole moment (direct output from G03), APT dipole, Mulliken dipole without electric field in Table 16. It is very clear that APT dipole is contributed to electronic polarizability very well, because the APT dipole is much smaller than dipole moment. But Mulliken dipole is larger than dipole moment at 6-311G, 6-311+G(2d), 6-311+G(3df), 6-311+G(3d2f) and LANL2DZ, it cannot represent electronic part well at those basis sets.

Table 16:   The comparison of dipole moment, APT dipole and Mulliken dipole without electric field at the B3LYP level.

no electric field (B3LYP)	Dipole moment	APT dipole	Mulliken dipole
6-311G	2.8765	0.159514	**3.373304**
6-311G(d)	2.6034	0.185058	1.660079
6-311+G	2.9311	0.182463	2.419225
6-311+G(d)	2.6716	0.243587	0.93931
6-311+G(2d)	2.5595	0.185182	**3.0296904**
6-311+G(2df)	2.5452	0.247732	1.1804818
6-311+G(3df)	2.5357	0.209746	**3.1015206**
6-311+G(3d2f)	2.5376	0.194249	**3.1624394**
LANL2DZ	2.9674	0.044939	**3.7838176**
CEP-31G	2.8633	0.524192	1.348365
CEP-121G	2.9241	0.56176	1.900735

Then it is as the same as the previous fitting of dipole moment and electric field, polarizability can be obtained easily. Because two kinds of dipole contribute to electronic part only, the obtained polarizability is called as the electronic polarizability. (See Table 17 and 18)

Table 17:   Mulliken dipole is fit with electric field (from -0.01 to 0.01 a.u.) and derives electronic polarizability at the B3LYP level.

Mulliken dipole	Fitting equation		α_e(debye/a.u.)	α_e (cm3)
6-311G	μ =	$797.56F^2 + 215.77F + 3.3734$	215.77	1.26E-23
6-311G(d)	μ =	$709.74F^2 + 222.06F + 1.6602$	222.06	1.29E-23
6-311+G	μ =	$801.95F^2 + 168.16F + 2.4304$	168.16	9.80E-24
6-311+G(d)	μ =	$336.26F^2 + 170.61F + 0.9527$	170.61	9.95E-24
6-311+G(2d)	μ =	$639.61F^2 + 190.57F + 3.0422$	190.57	1.11E-23
6-311+G(2df)	μ =	$555.59F^2 + 196.23F + 1.1929$	196.23	1.14E-23
6-311+G(3df)	μ =	$-1606.9F^2 + 167.54F + 3.123$	167.54	9.77E-24
6-311+G(3d2f)	μ =	$-1404.5F^2 + 172.79F + 3.1857$	172.79	1.01E-23
LANL2DZ	μ =	$357.76F^2 + 164.93F+ 3.7838$	164.93	9.62E-24
CEP-31G	μ =	$7.4405F^2 + 185.44F + 1.3484$	185.44	1.08E-23
CEP-121G	μ =	$23.877F^2 + 204.23F + 1.9008$	204.23	1.19E-23

Table 18:   APT dipole is fit with electric field (from -0.01 to 0.01 a.u.) and derives
electronic polarizability at the B3LYP level.

APT dipole	Fitting equation	α_e (debye/a.u.)	α_e (cm3)
6-311G	$\mu = 245.14F^2 + 189.49F + 0.1592$	189.49	1.10E-23
6-311G(d)	$\mu = 389.28F^2 + 177.78F + 0.1849$	177.78	1.04E-23
6-311+G	$\mu = 1017.8F^2 + 205.41F + 0.1774$	205.41	1.20E-23
6-311+G(d)	$\mu = 1580.7F^2 + 193.93F + 0.2377$	193.93	1.13E-23
6-311+G(2d)	$\mu = 1766F^2 + 189.15F + 0.1798$	189.15	1.10E-23
6-311+G(2df)	$\mu = 1747.2F^2 + 187.65F + 0.2423$	187.65	1.09E-23
6-311+G(3df)	$\mu = 2012.7F^2 + 185.85F + 0.2041$	185.85	1.08E-23
6-311+G(3d2f)	$\mu = 1998.7F^2 + 185.94F + 0.1885$	185.94	1.08E-23
LANL2DZ	$\mu = -1132.8F^2 + 148.82F - 0.0451$	148.82	8.68E-24
CEP-31G	$\mu = -454.06F^2 + 171.9F - 0.5254$	171.9	1.00E-23
CEP-121G	$\mu = -643.99F^2 + 200.23F - 0.563$	200.23	1.17E-23

Compare Table 17 to Table 18, it shows that the spread of electronic polarizability from Mulliken dipole is more dispersive than APT dipole by Pople's basis sets and effective core potential, because Mulliken charge is sensitive to the choice of basis sets and it usually is reasonable as small- or moderate-basis sets are used. So if we adopt the polarizability from APT dipole to calculate the dielectric constant, the larger basis sets should be used. And if we adopt the polarizability from Mulliken dipole to calculate the dielectric constant, the smaller basis sets should be used.

By applying Clausius-Mossotti equation we can combine the macroscopic amounts of dielectric constant with the microscopic amounts of polarizability.

$$\frac{\varepsilon_r - 1}{\varepsilon_r + 2} = \frac{n\alpha}{3\varepsilon_0} \tag{4.9}$$

Dielectric constant is obtained in eq. (4.10) by rearranging eq. (4.9). ρ is the density and M is the molecular weight.

$$\varepsilon_r = \frac{1 + 2A}{1 - A}$$
$$A = \frac{n\alpha}{3\varepsilon_0}, \; n = \frac{N}{V} = \frac{N_A \rho}{M} \tag{4.10}$$

Dielectric constants with respect to different basis sets are calculated and summarized in Table 19 and 20. The density is 1.99 g/cm^3 and Molecular weight is 76.6955 g/mol for Mg$_2$Si which are taken from experiment results.

Table 19:   Use APT charges to obtain electronic polarizability and dielectric

constant at the B3LYP level.

APT	α_e (debye/a.u.)	α_e(cm3)	dielectric constant
6-311G	189.49	1.10E-23	8.82
6-311G(d)	177.78	1.04E-23	7.32
6-311+G	205.41	1.20E-23	**11.86**
6-311+G(d)	193.93	1.13E-23	**9.53**
6-311+G(2d)	189.15	1.10E-23	**8.77**
6-311+G(2df)	187.65	1.09E-23	**8.56**
6-311+G(3df)	185.85	1.08E-23	**8.31**
6-311+G(3d2f)	185.94	1.08E-23	**8.32**
LANL2DZ	148.82	8.68E-24	4.94
CEP-31G	171.9	1.00E-23	6.71
CEP-121G	200.23	1.17E-23	**10.70**

Table 20:   Use Mulliken charges to obtain electronic polarizability and dielectric

constant at the B3LYP level.

Mulliken	α_e (debye/a.u.)	α_e(cm3)	dielectric constant
6-311G	215.77	1.26E-23	**14.95**
6-311G(d)	222.06	1.29E-23	**17.61**
6-311+G	168.16	9.80E-24	6.37
6-311+G(d)	170.61	9.95E-24	6.59
6-311+G(2d)	190.57	1.11E-23	8.99
6-311+G(2df)	196.23	1.14E-23	9.93
6-311+G(3df)	167.54	9.77E-24	6.31
6-311+G(3d2f)	172.79	1.01E-23	6.80
LANL2DZ	164.93	9.62E-24	6.09
CEP-31G	185.44	1.08E-23	**8.25**
CEP-121G	204.23	1.19E-23	**11.58**

The high frequency dielectric constant ε_∞ is 13.3* by experiment. The contribution of the high frequency dielectric constant is totally from electronic polarizability. From Table 19 no matter how to choose Pople's basis sets, the obtained dielectric constants are close to the experimental value when the larger basis sets are used (6-311+G, 6-311+G(d)…etc), and for effective core potential it shows the good result only at a larger basis set (CEP-121G), but LANL2DZ is unavailable here.

However, in Table 20 for Pople basis sets it shows good results corresponding to experimental value only when the smaller basis sets (6-311G, 6-311G(d)) are used. For ECP, it also shows that the available values are from CEP-series basis sets, but for LANL2DZ it shows a bad result. The results of Table 19 and 20 are vey correspondent to the theory mentioned earlier (in 2-2 charge population). The theory shows below:

1. Mulliken population analysis is affected largely by basis functions, and it usually is most useful for comparing trends in charge distributions, when small- or medium-size basis sets are used.

2. APT charge isn't directly related to the choice of a particular basis set, its basis set dependence stems only from the fact that the basis set can be incomplete. So the basis-set dependence is modest

4-1-4   Other methods (BLYP, M05 and M05-2X)

Now, we try other methods: BLYP, M05 and M05-2X. The process is the same as the previous B3LYP level.
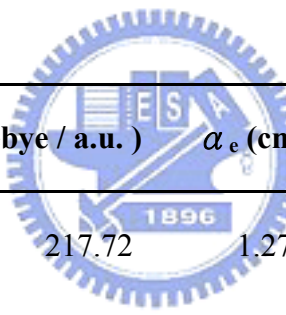
In Table 21, for the Pople's basis set, we show that the dielectric constant obtained from APT charge is in good agreement with experimental value (ε_∞ = 13.3) as the basis set is large enough (see larger bold-faced words) at the BLYP level. And for effective core potential it also shows that the dielectric constant is in good agreement with experimental value at a larger basis set (CEP-121G).

Table 21:   Use APT charges to obtain electronic polarizability and dielectric constant at BLYP level.

APT (BLYP)	α_e (Debye / a.u.)	α_e (cm3)	dielectric constant
6-311G	189.97	1.11E-23	8.89
6-311G(d)	181.66	1.06E-23	7.77
6-311+G	209.81	1.22E-23	**13.03**
6-311+G(2df)	197.76	1.15E-23	**10.21**
6-311+G(3d2f)	196.33	1.14E-23	**9.95**
LANL2DZ	138.64	8.08E-24	4.37
CEP-31G	163.09	9.51E-24	5.94
CEP-121G	184.83	1.08E-23	**8.17**

In Table 22 for Pople basis sets, the dielectric constant is fit well for a small basis set. However, for 6-311+G (2df) the dielectric constant is a good fit (see asterisk), it is contradictory to the unexpected results of Mulliken charge at a larger basis set. So we try the largest basis set (6-311+G (3d2f)) in order to check this contradiction. However, the dielectric constant at 6-311+G (3d2f) isn't a good fit. So we consider that it is a coincidence for the good result of 6-311+G (2df). And for ECP, it corresponds to the experimental value only at a larger basis set (CEP-121G).
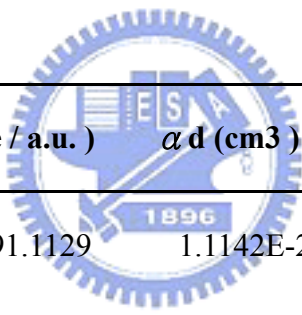
Table 22:　　Use Mulliken charges to obtain electronic polarizability and dielectric constant at the BLYP level.

Mulliken (BLYP)	α_e (Debye / a.u.)	α_e (cm3)	dielectric constant
6-311G	217.72	1.27E-23	**15.70**
6-311G(d)	222.99	1.30E-23	18.08
6-311+G	176.44	1.03E-23	7.17
6-311+G(2df)	202.41	1.18E-23	11.16*
6-311+G(3d2f)	184.22	1.07E-23	8.09
LANL2DZ	162.86	9.49E-24	5.92
CEP-31G	185.26	1.08E-23	8.23
CEP-121G	203.11	1.18E-23	**11.32**

In Table 23, for Pople basis sets it shows a good fit only at 6-311G and 6-311+G, but at a larger basis set the dielectric constant is much far from the experimental value. So Pople basis sets in the M05 level are unavailable for the APT derivation. There is no similar trend like B3LYP or BLYP in the M05 level. For the new M05 method it doesn't include enough parameters, so it isn't suited to use in our case. But for ECP, the dielectric constant is correspondent to the experimental value at larger basis sets (CEP-31G and CEP-121G).

Table 23: Use APT charges to obtain electronic polarizability and dielectric constant at the M05 level.

APT (M05)	α d (Debye / a.u.)	α d (cm3)	dielectric constant
6-311G	191.1129	1.1142E-23	9.0701*
6-311G(d)	174.7550	1.0188E-23	6.9982
6-311+G	192.6017	1.1229E-23	9.3070*
6-311+G(2df)	56.7148	3.3065E-24	1.8282
6-311+G(3d2f)	125.7389	7.3306E-24	3.7651
LANL2DZ	1274.8705	7.4325E-23	4.7766
CEP-31G	208.4698	1.2154E-23	**12.6489**
CEP-121G	200.1852	1.1671E-23	**10.6906**

In Table 24 for Pople basis sets, the dielectric constant is still not correspondent to experimental value, so those results are not also suited to analyses in our case. For ECP, it shows a good results only at CEP-31G..

Table 24: Use Mulliken charges to obtain electronic polarizability and dielectric constant at the M05 level.

Mulliken (M05)	α_e (Debye / a.u.)	α_e (cm3)	dielectric constant
6-311G	235.0190	1.3702E-23	26.9794
6-311G(d)	238.2464	1.3890E-23	30.8908
6-311+G	171.2971	9.9866E-24	6.6558
6-311+G(2df)	250.8102	1.4622E-23	67.3060
6-311+G(3d2f)	143.2398	8.3509E-24	4.6136
LANL2DZ	185.2729	1.0801E-23	8.2292
CEP-31G	208.2056	1.2138E-23	**12.5772**
CEP-121G	233.1315	1.3592E-23	25.0950

In Table 25 and 26 based on the M052X level, no matter APT charge or Mulliken charge both show bad results by Pople basis sets and ECP, although for APT charge the dielectric constant is similar at each basis set. Those bad results of M052X are very reasonable, because the new method – M052X is parameterized only for non-metals. But Mg atom is metal.

Table 25: Use APT charges to obtain electronic polarizability and dielectric constant at the M052X level.

APT (M052X)	α_e (Debye / a.u.)	α_e (cm3)	dielectric constant
6-311G	163.5600	9.5355E-24	5.9766
6-311G(d)	175.3025	1.0220E-23	7.0550
6-311+G	171.4508	9.9956E-24	6.6705
6-311+G(2df)	181.7957	1.0599E-23	7.7866
6-311+G(3d2f)	178.4675	1.0405E-23	7.3974
LANL2DZ	250.5412	1.4607E-23	65.7015
CEP-31G	129.6915	7.5610E-24	3.9372
CEP-121G	7.4667	4.3531E-25	1.0880

Table 26:   Use Mulliken charges to obtain electronic polarizability and dielectric constant at the M052X level.

Mulliken (M052X)	α_e (Debye / a.u.)	α_e (cm3)	dielectric constant
6-311G	224.2322	1.3073E-23	18.7371
6-311G(d)	229.1981	1.3362E-23	21.8616
6-311+G	178.5347	1.0409E-23	7.4050
6-311+G(2df)	194.3835	1.1333E-23	9.6043
6-311+G(3d2f)	150.9721	8.8017E-24	5.0735
LANL2DZ	166.0045	9.6781E-24	6.1794
CEP-31G	195.0367	1.1371E-23	9.7172
CEP-121G	219.9386	1.2822E-23	16.6282

Briefly, For Pople basis sets, there are good results from APT dipole by larger basis sets in the B3LYP and BLYP levels, and there are good results from Mulliken dipole by small basis sets in the B3LYP and BLYP levels. For ECP, no matter APT or Mulliken partial charge, there are good results by CEP-series basis sets at the B3LYP, BLYP and M05 levels .But for M052X it isn't suited to calculate in our case ,due to the fact that M052X is parameterized only for non-metals.

We conclude that in the present calculation for dielectric constant that M05 and M05-2X are not really better functionals than their original forms of B3LYP and BLYP.

4-1-5 Seebeck coefficient

Because the definition of Seebeck coefficient is

$$S_e = \lim_{\Delta T \to 0} \frac{\Delta V_p}{\Delta T} = \frac{dV_p}{dT} \tag{4.11}$$

Se is Seebeck coefficient, V_p is potential and T is absolute temperature.

From thermodynamic relation

Internal
energy

$$F = U - TS$$

Energy you can get from
the system's
environment by heating

Helmholtz
free energy

If we consider electric work, Helmholtz free energy can be written as

$$dF = -PdV - SdT + V_p dq \tag{4.12}$$

P is pressure, V_p is potential, V is volume, S is entropy, and q is charge.

From eq. (4.12), the below relations are obtained.

$$S = -\left(\frac{\partial F}{\partial T}\right)_{V,q} \quad , \quad P = -\left(\frac{\partial F}{\partial V}\right)_{T,q} \quad , \quad V_p = \left(\frac{\partial F}{\partial q}\right)_{T,V} \tag{4.13}$$

In order to obtain the Seebeck coefficient, we combine the relation of the eq. (4.13) with the definition of the eq. (4.11). Then it leads to

$$S_e = \frac{dV_p}{dT} = \frac{d\left(\frac{\partial F}{\partial q}\right)_{V,T}}{dT} \tag{4.14}$$

Now the dielectric constant ($\varepsilon_r = 11.86$) is taken from the APT dipole of 6-311+G basis set at the B3LYP level to calculate Seebeck coefficient. In first step, Helmholtz free energy at zero electric field is taken, and its unit is changed from

atomic unit to electron volt. Because we want to obtain the relation of the potential

and the temperature, the electron charge would be based on one atomic unit.

Therefore Helmholtz free energy with unit of electron volt is divided by unit

electron charge (See Table 27). Then the obtained result is fit with the temperature

from 300K to 800K. (See eq. 4.15)

Table 27:   Helmholtz free energy from B3LYP/6-311+G and the potential at one

unit electron charge (V).

B3LYP/6-311+G	300K	400K	500K	600K	700K	800K
Helmholtz energy (Hartree)	-689.656798	-689.669068	-689.681888	-689.695150	-689.7087777	-689.7227217
Helmholtz energy (eV)	-18766.7160	-18767.0499	-18767.3988	-18767.7596	-18768.13048	-18768.50992
potential (at unit charge,V)	-18766.7160	-18767.0499	-18767.3988	-18767.7596	-18768.13048	-18768.50992

The fitting equation via potential and temperature from Table 27 is listed below.

$$V_p = 6 \times 10^{-07} T^2 + 0.003T + 18766 \qquad (4.15)$$

Then the Seebeck coefficient is

$$S_e = \frac{dV_p}{dT} = 1.2 \times 10^{-06} T + 0.003 \qquad (4.16)$$

However, eq. (4.16) is due to molecule Mg_2Si is at zero electric field and it is

represented as gas phase. But the Mg_2Si material is a polar solid so that the electric

potential inside this dielectric should be divided by the calculated dielectric constant

of 11.86 from gas phase[9], and then actually the Seebeck coefficient of Solid state is

given as

$$S_e = 1 \times 10^{-7} \ T + 2.52 \times 10^{-4} \qquad (4.17)$$

In Fig. 19 it shows the fitting profiles from solid-state, gas-phase and Material studio 4.0 of Mg_2Si and in Fig. 18[32] it shows the experimental results. Compare Fig. 19 to Fig. 20, we find that our solid-state case agrees with experimental results of non-BN coated, and also find our fitting result is linear even at higher temperature. But in Fig. 20 the Seebeck coefficient of the BN coated fitting decreases as temperature increasing, which may originate in the effect thermal excitation of carriers across the gap from the conduction band[33]. However, in our case because we don't consider energy band structure theory but directly based on thermodynamic method, it doesn't show that Seebeck coefficient decrease at high temperature.
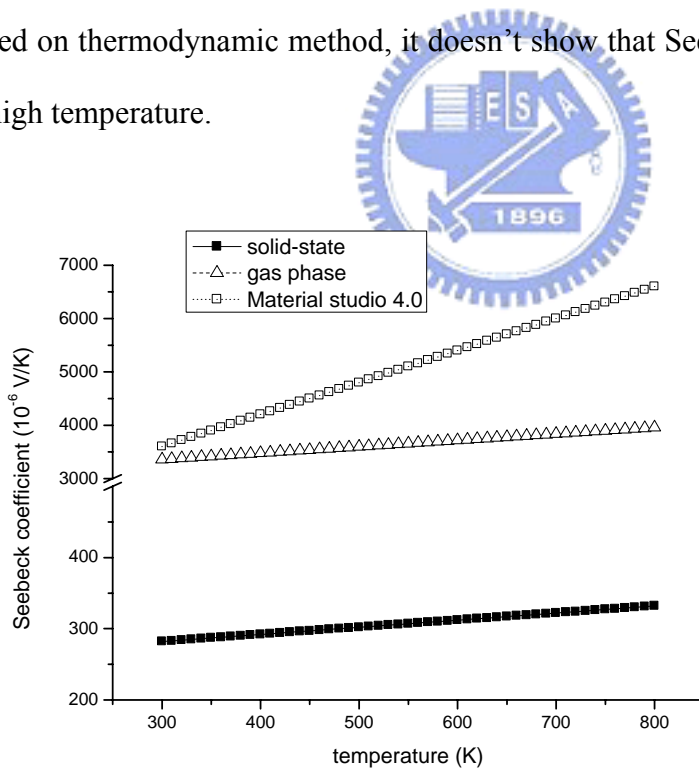
Fig. 19   The fitting profiles from solid-state, gas phase and Material studio 4.0
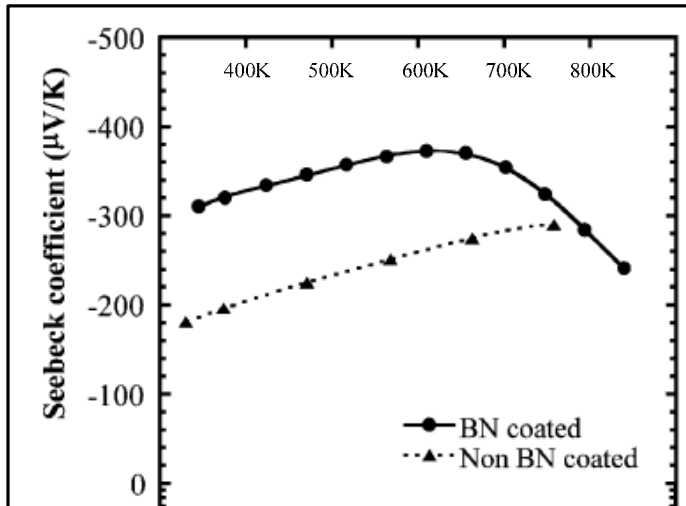
Fig. 20.   Seebeck coefficient of the grown ingot over the range is from 345K to 840 K[32]. BN coated means encapsulated sample with a boron nitride (BN)-based anti-adhesion coating.

A summary of Seebeck coefficient is listed in Table 28.

Table 28:   Seebeck coefficients are obtained from gas phase, solid state and Material studio 4.0[9] respectively, and compare to experiment value.

B3LYP/6-311+G	fitting equation	Se (µV/K) 300K	Se (µV/K) 800K
gas phase	$S_e = 1.2*E\text{-}06\ T + 0.003$	3360	3960
solid state	$S_e = 1*E\text{-}07\ T + 2.52*E\text{-}04$	**284**	**334**
material studio 4.0[9]	$S_e = 6*E\text{-}06\ T + 0.0018$	3600	6600
experimental value[32]		180	280

In Table 28 it shows clearly that Seebeck coefficient agrees with experiment value by our treatment of solid state very well. But for Material studio 4.0 based on the energy band structure theory, the Seebeck coefficient that is similar to our gas phase case isn't fitted to experimental value. So we can conveniently obtain more accurate Seebeck coefficient from the thermodynamic method with the present new scheme.

4-2 Iron Disilicide (FeSi$_2$)

4-2-1 Polarizability and dielectric constant

Because Fe atom is a transition metal which belongs to the system of the heavy atoms, we would consider the relativistic effect for FeSi$_2$ molecule, and then we adopt the effective core potential (ECP). Here, LANL2DZ, CEP-31G and CEP-121G basis sets and 6-311+G(2d), 6-311+G(2df), 6-311+G(3df) and 6-311+G(3d2f) are used, besides 6-311G, 6-311G(d), 6-311+G and 6-311+G(d) basis sets. Furthermore, we try other methods such as BLYP, M05 and M05-2X, in order to compare with B3LYP mentioned previously.

There are polarizabilities and dielectric constants calculated with different basis sets from APT charge at B3LYP level in Table 29. The experimental value of high-frequency dielectric constant is 27.6[34]. We compare this experimental value with Table 29. Basis sets are in two parts: one is Pople style basis set, and the other is effective core potential (ECP). The dielectric constants from Pople style basis sets are in good agreement with experimental value, when basis sets are larger (6-311+G ~ 6-311+G (3d2f)). But when basis sets aren't enough large, the dielectric constants aren't good fits (6-311G and 6-311G(d)). Those results of the derivation of APT charge match the phenomenon that the basis-set dependence is modest for these APT charges, and those APT charges usually converge at the larger basis set. Expectably, for Pople basis sets of APT part, the dielectric constants of FeSi$_2$ show the same trend as of Mg$_2$Si at the B3LYP level. The second part of Table 29: effective core potential, CEP-31G is Stevens/Basch/Krauss ECP split valance, CEP-121G is Stevens/Basch/Krauss ECP triple-split basis, LANL2DZ is

Los Alamos ECP plus DZ on Na-La. The dielectric constant is in good agreement with experimental value only at CEP-31G and CEP-121G, and it is unreasonable for LANL2DZ.

Table 29: Electronic polarizability and dielectric constants are obtained from APT partial charge by Pople style basis sets and ECP (effective core potential) at the B3LYP level.

APT (B3LYP)	α_e (debye/a.u.)	α_e(cm3)	dielectric constant
6-311G	438.8397669	2.5584E-23	5.601
6-311G(d)	101.3604885	5.9093E-24	6.923
6-311+G	170.101198	9.9169E-24	**30.323**
6-311+G(d)	174.98552	1.0202E-23	**24.554**
6-311+G(2d)	175.4081556	1.0226E-23	**24.171**
6-311+G(2df)	171.9406231	1.0024E-23	**27.806**
6-311+G(3df)	170.7639673	9.9555E-24	**29.357**
6-311+G(3d2f)	171.5035795	9.9987E-24	**28.360**
LANL2DZ	151.3419434	8.8232E-24	335.790
CEP-31G	170.3221211	9.9298E-24	**29.993**
CEP-121G	174.8990718	1.0197E-23	**24.634**

In Table 30, dielectric constants are derived from Mulliken partial charge by Pople basis sets and ECP at B3LYP level. It is found that dielectric constants with Pople basis sets are almost incorrect, even with smaller basis sets (ex. 6-311G), those results are very different from Mg_2Si, because in Mg2Si the dielectric constant is fit well with Mulliken part when the basis set is smaller. Although the dielectric constant of 6-311+G (3df) is a good fit, don't forget that Mulliken charges show incorrect results when basis sets become larger and larger.

The second part of Table 30 shows the ECP. For APT part, no matter CEP-series basis sets or LANL2DZ, the dielectric constants from Mulliken partial charge aren't correspondent to the experimental value.

Table 30: Electronic polarizability and dielectric constants are obtained from Mulliken partial charge by Polpe style basis sets and ECP at B3LYP level.

Mulliken(B3LYP)	α_e (debye/a.u.)	α_e(cm3)	dielectric constant
6-311G	218.7619168	1.2754E-23	10.9341
6-311G(d)	211.2409253	1.2315E-23	11.8249
6-311+G	192.654567	1.1232E-23	15.4648
6-311+G(d)	194.4171493	1.1335E-23	14.9805
6-311+G(2d)	188.1928805	1.0972E-23	16.906
6-311+G(2df)	194.2154369	1.1323E-23	15.0338
6-311+G(3df)	172.9539878	1.0083E-23	26.6154*
6-311+G(3d2f)	185.9308199	1.0840E-23	17.7844
LANL2DZ	164.6645681	9.5999E-24	42.2815
CEP-31G	179.8362233	1.0484E-23	20.8801
CEP-121G	209.1469583	1.2193E-23	12.1152

We would like to compare B3LYP with BYLP. Unfortunately, APT part is in Table 31, no matter Pople basis sets or ECP aren't correspondent to the experimental value. It is very different from Mg_2Si at the BLYP level. For APT part of Mg_2Si at the BLYP level it shows the similar result with the B3LYP level, however, for $FeSi_2$ it can't perform very well at the BLYP level. So we think that the BLYP level isn't good for transition metals (Fe) and the B3LYP level is good for all metals. Although the results aren't good, we still can discover that the APT charges would converge at larger basis sets (see the dielectric constants of 6-311+G(2df), 6-311+G(3df) and 6-311+G(3d2f)).

Table 31: Electronic polarizability and dielectric constants are obtained from APT partial charge by Pople style basis sets and ECP at BLYP level.

APT(BLYP)	α_e (debye/a.u.)	α_e(cm3)	dielectric constant
6-311G	164.3716048	9.5829E-24	43.242
6-311G(d)	123.8514228	7.2205E-24	13.880
6-311+G	120.2782315	7.0122E-24	12.130
6-311+G(d)	98.75743785	5.7576E-24	6.493
6-311+G(2d)	122.1128539	7.1192E-24	12.978
6-311+G(2df)	115.0096953	6.7051E-24	10.155
6-311+G(3df)	116.5465518	6.7947E-24	10.672
6-311+G(3d2f)	115.9894413	6.7622E-24	10.479
Lanl2DZ	104.7655862	6.1078E-24	7.557
CEP-31G	200.6077994	1.1695E-23	13.562
CEP-121G	202.4520272	1.1803E-23	13.207

In Table 32, it is Mulliken part at the BLYP level. For Pople basis sets and ECP all the dielectric constants aren't in agreement with the experimental value. It is proven again that the BLYP level isn't good for transition metal.

Table 32: Electronic polarizability and dielectric constants are obtained from Mulliken partial charge by Polpe style basis sets and ECP at BLYP level.

Mulliken(BLYP)	α_e (debye/a.u.)	α_e(cm3)	dielectric constant
6-311G	206.0252185	1.2011E-23	12.5903
6-311G(d)	200.8239198	1.1708E-23	13.5187
6-311+G	201.9861676	1.1776E-23	13.2942
6-311+G(d)	200.0602943	1.1664E-23	13.6721
6-311+G(2d)	192.327985	1.1213E-23	15.5593
6-311+G(2df)	198.1872504	1.1554E-23	14.0704
6-311+G(3df)	175.9940821	1.0260E-23	23.6641*
6-311+G(3d2f)	190.1571752	1.1086E-23	16.2292
LANL2DZ	180.3981365	1.0517E-23	20.5377
CEP-31G	209.6128179	1.2220E-23	12.0488
CEP-121G	215.952351	1.2590E-23	11.2421

APT part is in Table 33. For Pople basis sets, the dielectric constants isn't correspondent to experimental value at larger basis sets, and results of 6-311G(d) and 6-311+G are available. But remember that it is available for APT charges at larger basis sets, and the APT charge would converge at so larger basis sets. For ECP, the dielectric constant is suited by CEP-121G, but still isn't fit by LANL2DZ. In summary, a new M05 method isn't parameterized including the perturbation of electric field for APT partial charge by Pople basis sets, so it can't show good results for dielectric constants.

Table 33:   Electronic polarizability and dielectric constants are obtained from APT

partial charge by Pople style basis sets and ECP at M05 level.

APT (M05)	α_e (debye/a.u.)	α_e(cm3)	dielectric constant
6-311G	185.3881174	1.0808E-23	18.013
6-311G(d)	170.0339605	9.9130E-24	30.425*
6-311+G	171.3739073	9.9911E-24	28.529*
6-311+G(d)	158.1809548	9.2219E-24	87.550
6-311+G(2d)	159.1270821	9.2771E-24	75.255
6-311+G(2df)	158.2241789	9.2245E-24	86.897
6-311+G(3df)	158.757276	9.2555E-24	79.603
6-311+G(3d2f)	159.2135302	9.2821E-24	74.309
LANL2DZ	187.5445192	1.0934E-23	17.146
CEP-31G	198.8308091	1.1592E-23	13.930
CEP-121G	174.0778142	1.0149E-23	**25.427**

Mulliken part is in Table 34. For Pople basis sets the dielectric constants aren't good fits, although the results of 6-311+G (3df) and 6-311+G (3d2f) are good. Remember again that for Mulliken charge it is available only at a small basis set, so the results of 6-311+G (3df) and 6-311+G (3d2f) are coincidences. It is proven again that M05 isn't parameterized including the perturbation of electric field for Mulliken partial charge by Pople basis sets. For ECP the dielectric constant is correspondent to the experimental value in LANL2DZ, but is unavailable in CEP-series basis sets.

Table 34: Electronic polarizability and dielectric constants are obtained from Mulliken partial charge by Polpe style basis sets and ECP at M05 level.

Mulliken (M05)	α_e (debye/a.u.)	α_e(cm3)	dielectric constant
6-311G	206.6927906	1.2050E-23	12.4841
6-311G(d)	197.005792	1.1485E-23	14.3389
6-311+G	191.1609346	1.1145E-23	15.91
6-311+G(d)	188.260118	1.0976E-23	16.8816
6-311+G(2d)	165.6299061	9.6562E-24	39.4238
6-311+G(2df)	161.8357916	9.4350E-24	54.1323
6-311+G(3df)	136.4056193	7.9524E-24	26.1169*
6-311+G(3d2f)	136.3527899	7.9494E-24	26.026*
LANL2DZ	174.0730115	1.0148E-23	**25.4314**
CEP-31G	197.1738857	1.1495E-23	14.2999
CEP-121G	204.8341548	1.1942E-23	12.7865

In Table 35 and 36, all information is based on the M052X level. No matter APT part or Mulliken part shows bad results of dielectric constants, the simple interpretation for that is M052X is parameterized only including nonmetals. But we still find that APT charge would converge at a larger and larger basis set.

Table 35: Electronic polarizability and dielectric constants are obtained from APT partial charge by Pople style basis sets and ECP at the M05-2X level.

APT (M05-2X)	α_e (debye/a.u.)	α_e(cm3)	dielectric constant
6-311G	300.4698529	1.7517E-23	7.100
6-311G(d)	208.9740619	1.2183E-23	12.140
6-311+G	190.7575098	1.1121E-23	16.036
6-311+G(d)	189.8690146	1.1069E-23	16.324
6-311+G(2d)	189.8738173	1.1070E-23	16.322
6-311+G(2df)	190.7623125	1.1121E-23	16.035
6-311+G(3df)	190.6854697	1.1117E-23	16.059
6-311+G(3d2f)	191.4010685	1.1159E-23	15.836
LANL2DZ	192.6209483	1.1230E-23	15.474
CEP-31G	83.17755513	4.8493E-24	4.589
CEP-121G	126.1855236	7.3566E-24	15.278

Table 36: Electronic polarizability and dielectric constants are obtained from Mulliken partial charge by Polpe style basis sets and ECP at the M05-2X level.

Mulliken (M05-2X)	α_e (debye/a.u.)	α_e(cm3)	dielectric constant
6-311G	256.621416	1.4961E-23	8.408
6-311G(d)	247.7364644	1.4443E-23	8.82
6-311+G	230.6773573	1.3448E-23	9.875
6-311+G(d)	109.8660287	6.4052E-24	8.695
6-311+G(2d)	156.9322589	9.1492E-24	112.19
6-311+G(2df)	208.4649782	1.2154E-23	12.214
6-311+G(3df)	68.81755225	4.0121E-24	3.461
6-311+G(3d2f)	64.26941756	3.7469E-24	3.18
LANL2DZ	190.8343526	1.1126E-23	16.012
CEP-31G	196.5687484	1.1460E-23	14.442
CEP-121G	211.5819153	1.2335E-23	11.78

In summary, for Pople basis sets in $FeSi_2$ the dielectric constants from APT partial charge are in good agreement with the experimental value only at the B3LYP level and from Mulliken partial charge are unavailable at all levels (B3LYP, BLYP, M05 and M052X). For ECP based on APT partial charge, it is also performs well only by CEP-series basis sets at the B3LYP, M05 levels. For the BLYP level, it is due to the fact that BLYP level isn't suited to calculation of transition metals, the dielectric constants don't agree with the experimental value. For the M052X level, because it is parameterized only including non-metals, the results are all unavailable.

4-2-2 Seebeck coefficient

Here B3LYP/6-311+G(2df) in Table 29 is adopted because the dielectric constant ($\varepsilon_r = 27.806$) is much closer to experimental value ($\varepsilon_\infty = 27.6$). In Table 37, Helmholtz energy and potential with unit charge in different temperatures are listed. Then we fit potentials with temperatures in Fig. 21. which shows a line of gas phase which is from the fitting of potentials and temperatures directly and a line of solid state which is from the fitting of gas phase divided by the calculated dielectric constant ($\varepsilon_r = 27.806$), because the $FeSi_2$ material is a polar solid so that the electric potential inside that.

In Fig. 22[35], it shows the experimental results, and from the undoped fitting by squares, it is in good agreement with the line of solid state in our case. Moreover, Ref. 35 also indicates calculated results based on the energy band structure with the local density approximation using Slater's $X\alpha$ potential, and it shows the worse result than solid state by our method in Table 38.

We make a small summary in Table 38. Seebeck coefficients in 300K or in

900K are more correspondent to the experimental value than calculation results from Ref. 35. However, in our solid state case the fitting equation is linear, and the Seebeck coefficient increases at the higher temperature. In experimental values and calculation results from Ref. 35, Seebeck coefficient decreases at the high temperature. That is due to consideration of the thermal excitation of carriers in Ref. 35, but in our case it is based on the thermodynamic method.

Table 37:   The Helmholtz free energy from B3LYP/6-311+G and the potential at one unit electron charge (V).

B3LYP/ 6-311+G(2df)	300K	400K	500K	600K	700K	800K	900K
Helmholtz energy (Hartree)	-1842.6875	-1842.6996	-1842.7122	-1842.7252	-1842.7386	-1842.7523	-1842.7663
Helmholtz energy (eV)	-50142.6124	-50142.9407	-50143.2835	-50143.6380	-50144.0024	-50144.3752	-50144.7555
potential (at unit charge , V)	-50142.6124	-50142.9407	-50143.2835	-50143.6380	-50144.0024	-50144.3752	-50144.7555
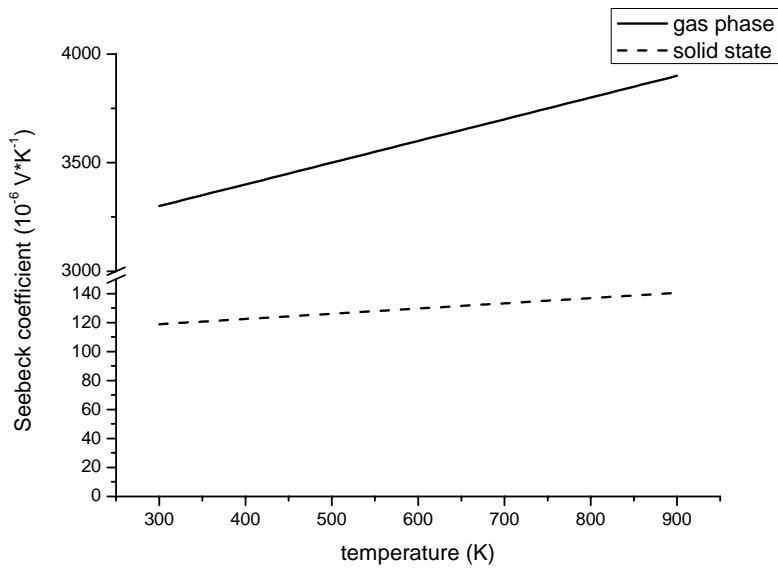
Fig. 21   The fitting profiles from solid-state, gas phase.
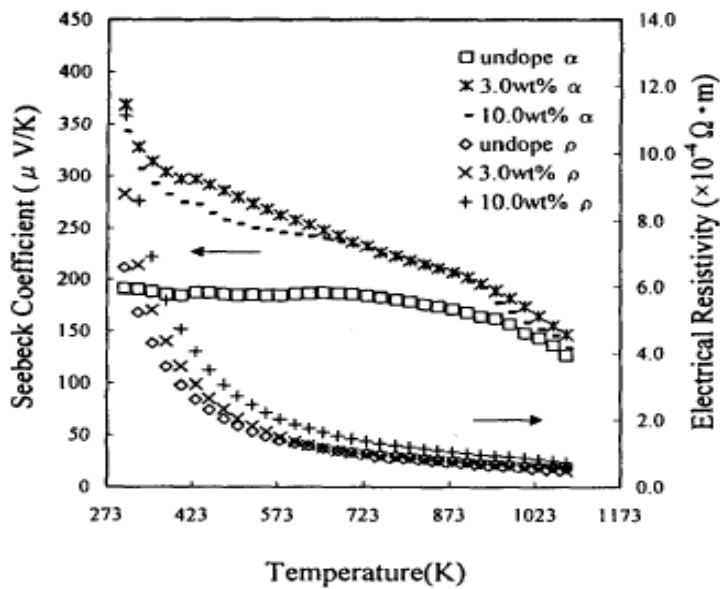
Fig. 22   Seebeck coefficient of FeSi$_2$ and Electrical resistivity of the undoped and

doped Yb$_2$O$_3$.

Table 38: Seebeck coefficients are obtained from gas phase, solid state, and compare to experimental values[35] and calculated results[35].

B3LYP/6-311+G	fitting equation	Se (µV/K) 300K	Se (µV/K) 900K
gas phase	Se = 1E-06T+0.003	3300.00	3900.00
solid state	Se= 3.6E-08T+1.08E-04	**118.80**	**140.40**
experimental value[35]		**190.00**	**170.000**
calculated results[35]		1000.00	380.000

4-3 Silicon Germanium (SiGe)

Bulk SiGe crystals have the application to photo-detectors, X-ray and neutron monochromators, etc. and SiGe crystals are also well-known materials for thermoelectric applications, especially perform well at higher temperature. Now, SiGe has attracted more interests in environmental compatibility.

4-3-1 Dielectric Constant

Here, we follow the previous procedure as we have done for Mg_2Si and $FeSi_2$. Three levels are used respectively: B3LYP, BLYP and M05. Basis sets are classified as two parts: Pople basis sets (series of 6-311G, 6-311G(d)…,etc) and effective core potential (LANL2DZ, CEP-31G and CEP-121G).

It is based on APT partial charge and the B3LYP level in Table 39. The dielectric constant by experiment is 13.95[36]. It performs well at larger Pople basis sets, and corresponds to theory of APT charge. For ECP, CEP-31G and CEP-121G shows good fits, especially for LANL2DZ it also performs very well. Those results are similar to Mg_2Si and $FeSi_2$.

Table 39:   Electronic polarizability and dielectric constants are obtained from APT

partial charge by Polpe style basis sets and ECP at the B3LYP level.

APT (B3LYP)	α_e (Debye / a.u.)	α_e (cm3)	dielectric constant
6-311G	423.8073893	2.47E-23	6.193
6-311G(d)	459.6833831	2.68E-23	5.913
6-311+G	1401.661151	8.17E-23	4.439
6-311+G(d)	262.3221931	1.53E-23	**10.442**
6-311+G(2df)	243.7502428	1.42E-23	**12.289**
6-311+G(3d2f)	235.076609	1.37E-23	**13.571**
LANL2DZ	222.4695831	1.30E-23	**16.345**
CEP-31G	280.0824909	1.63E-23	**9.311**
CEP-121G	278.8289923	1.63E-23	**9.377**

It is based on Mulliken partial charge and B3LYP level in Table 40. It shows good results at small Pople basis sets (6-311G and 6-311G(d)) which corresponds to the theory of Mulliken charge. And for all ECP it shows very good results.

Table 40:   Electronic polarizability and dielectric constants are obtained from Mulliken partial charge by Polpe style basis sets and ECP at the B3LYP level.

Mulliken(B3LYP)	α_e (Debye / a.u.)	α_e (cm3)	dielectric constant
6-311G	234.0008094	1.36E-23	**13.758**
6-311G(d)	226.2636975	1.32E-23	**15.355**
6-311+G	207.3027305	1.21E-23	22.956
6-311+G(d)	228.8955643	1.33E-23	14.756*
6-311+G(2df)	208.4361622	1.22E-23	22.226
6-311+G(3d2f)	192.6017376	1.12E-23	43.409
LANL2DZ	246.0747383	1.43E-23	**12.002**
CEP-31G	249.7295751	1.46E-23	**11.589**
CEP-121G	265.6984747	1.55E-23	**10.191**

It is based on APT partial charge and BLYP level in Table 41. No matter Pople basis sets or ECP, dielectric constants are in good agreement with the experimental value. Those results are similar to in Mg_2Si where the results of the B3LYP and BLYP level are almost the good.

Table 41:　Electronic polarizability and dielectric constants are obtained from APT partial charge by Polpe style basis sets and ECP at the BLYP level.

APT (BLYP)	α_e (Debye / a.u.)	α_e (cm3)	dielectric constant
6-311G	244.9461093	1.43E-23	12.139
6-311G(d)	259.6086808	1.51E-23	10.659
6-311+G	240.599687	1.40E-23	12.713
6-311+G(d)	253.1538835	1.48E-23	11.239
6-311+G(2df)	232.2334245	1.35E-23	14.082
6-311+G(3d2f)	224.8565133	1.31E-23	15.703
LANL2DZ	219.1653416	1.28E-23	17.360
CEP-31G	275.6784365	1.61E-23	9.552
CEP-121G	272.7488038	1.59E-23	9.726

It is based on Mulliken partial charge and BLYP level in Table 42. It shows good results at small Pople basis sets, and it also performs well at CEP-31G, CEP-121G and LANL2DZ.

Table 42:   Electronic polarizability and dielectric constants are obtained from Mulliken partial charge by Polpe style basis sets and ECP at the BLYP level.

Mulliken(BLYP)	α_e (Debye / a.u.)	α_e (cm3)	dielectric constant
6-311G	275.6208044	1.61E-23	**9.556**
6-311G(d)	259.2244667	1.51E-23	**10.691**
6-311+G	251.3384718	1.47E-23	**11.420**
6-311+G(d)	230.7638055	1.35E-23	**14.368**
6-311+G(2df)	209.9634133	1.22E-23	21.328
6-311+G(3d2f)	193.0291758	1.13E-23	42.211
LANL2DZ	245.3975609	1.43E-23	**12.084**
CEP-31G	253.4324388	1.48E-23	**11.211**
CEP-121G	267.9461273	1.56E-23	**10.035**

It is based on APT partial charge and the M05 level in Table 43. Dielectric constants are fit to larger Pople basis sets, but for CEP-31G, CEp-121G and LANL2DZ they show unavailable results.

Table 43:   Electronic polarizability and dielectric constants are obtained from APT partial charge by Polpe style basis sets and ECP at the M05 level.

APT (M05)	α_e (Debye / a.u.)	α_e (cm3)	dielectric constant
6-311G	131.1418858	7.65E-24	**9.225**
6-311G(d)	246.2476346	1.44E-23	**11.982**
6-311+G	226.4077778	1.32E-23	**15.320**
6-311+G(d)	248.7306184	1.45E-23	**11.698**
6-311+G(2df)	227.118574	1.32E-23	**15.153**
6-311+G(3d2f)	225.9131021	1.32E-23	**15.440**
LANL2DZ	334.9050437	1.95E-23	7.443
CEP-31G	1378.272116	8.04E-23	4.448
CEP-121G	786.0060438	4.58E-23	4.885

It is based on Mulliken partial charge and M05 level in Table 44. It performs well at small Pople basis sets. And dielectric constants are correspondent to the experimental value at CEP-31G, CEP-121G and LANL2DZ. It is unlike effective core potential in Table 43 that dielectric constants are unavailable with CEP-31G, CEP-121G and LANL2DZ.

Table 44: Electronic polarizability and dielectric constants are obtained from Mulliken partial charge by Polpe style basis sets and ECP at the M05 level.

Mulliken(M05)	α_e (Debye / a.u.)	α_e (cm3)	dielectric constant
6-311G	270.6452315	1.58E-23	**9.857**
6-311G(d)	264.6947153	1.54E-23	**10.264**
6-311+G	252.5391409	1.47E-23	**11.299**
6-311+G(d)	240.7773861	1.40E-23	**12.688**
6-311+G(2df)	225.543296	1.31E-23	**15.531**
6-311+G(3d2f)	224.2801921	1.31E-23	**15.852**
LANL2DZ	246.583822	1.44E-23	**11.942**
CEP-31G	242.5015469	1.41E-23	**12.452**
CEP-121G	263.0329892	1.53E-23	**10.388**

In summary, for Pople basis sets and effective core potential in the SiGe case, they both show expectable, better results no matter at the B3LYP or BLYP or M05 level. It is also proven that our method can applied to calculate dielectric constant.

4-3-2   Seebeck Coefficient

Here B3LYP/6-311+G(3d2f) in Table 39 is adopted because the dielectric constant (ε_r = 13.571) is much closer to experimental value (ε_∞ = 13.95). In Table 45, Helmholtz energy and potential with a unit charge in different temperatures are listed. Then we fit potentials with temperatures in Fig. 23 which shows a line of gas phase which is from the fitting of potentials and temperatures directly and a line of solid state which is from the fitting of gas phase divided by the calculated dielectric constant (ε_r = 13.571), because the SiGe material is a polar solid so that the electric potential inside that.

Fig. 24 shows the Seebeck coefficient of SiGe single crystals with different directs as a function of temperature[33]. Although the Seebeck coefficient in our solid-state case has little different from the experimental value of Fig. 24, our results locate at same order of magnitude with the experimental value. The results of solid-state case are acceptable. But Fig. 24 shows that Seebeck coefficient decreases at higher temperature, it is very different from our calculations which increase at higher temperature. The reason is the same as the previous discussion that Seebeck coefficient is observed to decrease at high temperature which may originate in the effect of thermal excitation of carriers across the gap from the conduction band[33]. However, our case is based on thermodynamic method than consideration about carrier motion of the energy band. So Fig. 23 shows linear lines than curves down.

Table 45: The Helmholtz free energy from B3LYP/6-311+G(3d2f) and the potential at one unit electron charge (V).

B3LYP/6-311+G(3d2f)	300	400	500	600
Helmholtz energy(Hartree)	-2366.4619	-2366.4719	-2366.4822	-2366.4928
Helmholtz energy(eV)	-64394.768	-64395.039	-64395.32	-64395.608
potential (at unit charge , V)	-64394.768	-64395.039	-64395.32	-64395.608

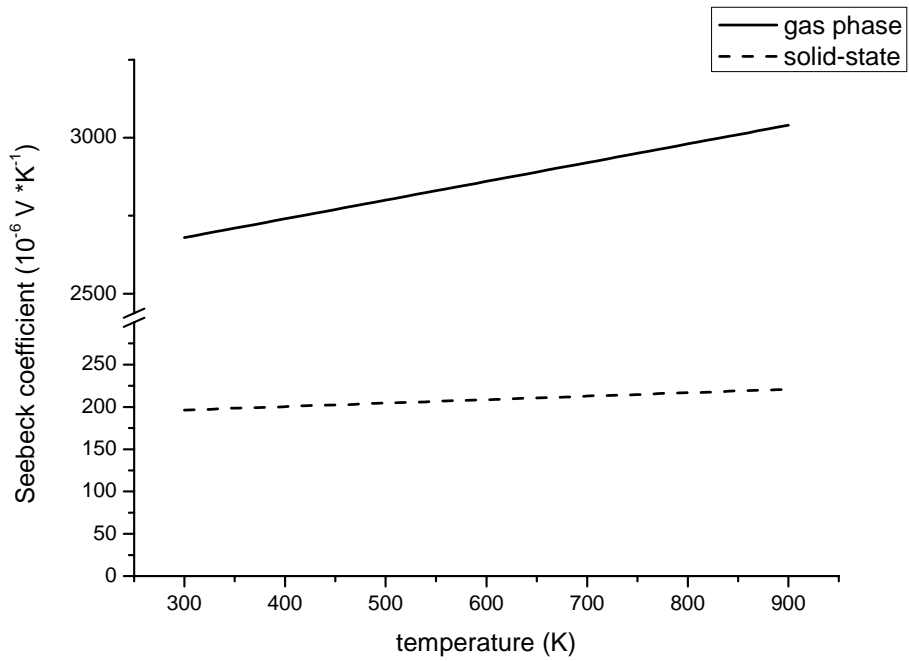| B3LYP/6-311+G(3d2f)	700	800	900
Helmholtz energy(Hartree)	-2366.5036	-2366.5147	-2366.5259
Helmholtz energy(eV)	-64395.903	-64396.203	-64396.508
potential (at unit charge , V)	-64395.903	-64396.203	-64396.508

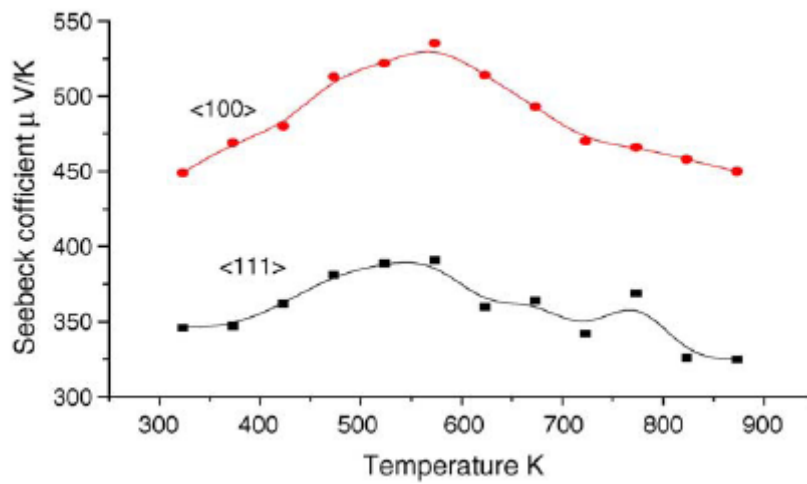Fig. 23   The fitting profiles from solid-state, gas phase.

Fig. 24   The Seebeck coefficient of SiGe single crystals with different direct is plotted against the temperature[33].

We make a small summary in Table 46 Seebeck coefficients in 300K or in 900K are correspondent to the experimental value for the solid-state case. However, in our solid state case the fitting equation is linear, and the Seebeck coefficient increases at the higher temperature. In experimental values, Seebeck coefficient decreases at the high temperature. That is due to consideration of the thermal excitation of carriers, but in our case it is based on the thermodynamic method.

Table 46:   Seebeck coefficients are obtained from gas phase, solid state, and compare to experimental values with different direct [33].

B3LYP/6-311+G(3d2f)	fitting equation	S_e (μV/K) 300K	S_e (μV/K) 900K
gas phase	$S_e = 6*E-7T +0.0025$	2680.0	3040.0
solid state	$S_e = 4.1E*-8T+1.84*E-4$	196.3	220.9
experimental value <100>		445.0	430.0
experimental value <111>		345.0	325.0

Chapter 5   Conclusion

We have developed the new method to study the thermoelectric effect based on thermodynamic theory for the system in the presence of an electric field. Three semiconductor thermoelectric materials, Mg_2Si, $FeSi_2$ and SiGe, are investigated as a demonstration of the present new method. Since thermodynamics can be considered as an exact theory in which all microscopic quantities are systematically averaged out so that it is possible to perform a more accurate calculation than the conventional energy band structure theory.

We have proposed the way to calculate electric polarizability directly by varying electric field. We start with calculating net charge change against electric field, but use equilibrium geometry at zero electric field to compute dipole momentum change only due to electronic polarization. In such way, we have obtained the electronic polarizability, and then inserting it into the Clausis-Mossotti equation leads to dielectric constant for bulk matter as it is required. We have employed two kinds of charges, APT and Mulliken types of charge. It is found that APT charge which converges to the reasonable and stable value as basis sets becoming large, so that the electronic polarizability calculated from APT charge converges systematically with increase basis sets. However, the electronic polarizability calculated from Mulliken charge does not show systematically converges, and it shows some good results in the certain extent only for a small or medium basis set. We have tried four functionals in DFT method: B3LYP, BLYP, M05 and M052X, and two types of basis sets: Pople basis sets including of 6-311G, 6-311G(d), 6-311+G...etc, and effective core potential including of CEP-31G, CEP-121G and LANL2DZ. Simulation results are summarized as follows:

1. B3LYP can simulate APT or Mulliken partial charges which can lead to good results for the calculation of dielectric constants, no matter by Pople basis sets or by Effective core potential.

2. BLYP is not good only for transition metals, and but it is good for the other metals.

3. M05 is the new method which may not is parameterized including enough information of the perturbation of electric fields in partial charges, so the results are unfavorable for computing electric polarizability.

4. M052X is parameterized only good for non-metals, so it is not good for the present case.

   Thermodynamic theory is a good tool for discussing thermoelectric effects, especially for Seebeck coefficient. The importance of evaluating Seebeck coefficient is the relation of electric potential and temperature, and the considerations for dielectric properties of solid-state material. The present method presents an alternative way to compute the Seeback coefficient, and it seems a better method in accuracy as well as in simplicity than the carrier motion of the conventional energy band structure theory. This can be easily seen from three examples that can for Mg_2Si Seebeck coefficient at 300K is 284 µV/K is in good agreement with experimental value 180 µV/K, but the result of material studio 4.0 shows 3600 µV/K. Equally, in 800K it is 334 µV/K is well suited with experimental value 280 µV/K, but the result of material studio 4.0 shows 6600 µV/K. The same situation occurs in the case of $FeSi_2$ and SiGe. Simulated Seebeck coefficients all are proven that our method provides a convenient and accurate calculation for Seebeck coefficient. Moreover, Seebeck coefficient from our case increases at high

temperature, but it decreases at high temperature by experiment. The difference is due to the fact that our method is based on thermodynamic theory than carrier motion of the energy band, but the experimental phenomenon originates in the effect of thermal excitation of carriers across the band gap.

Although we succeed in simulating dielectric constants and Seebeck coefficients for $FeSi_2$, Mg_2Si and SiGe, there are still many thermoelectric materials in the world to be investigated in the future. For example, by far Bi_2Te_3 is the most important thermoelectric material, and we also can try many atoms of the molecule by our method in the future. Now, the most promising approach for the increase of the thermoelectric efficiency is to create highly doped, we will definitely study those doped materials in the future.

Reference

1. Terasaki, I., Introduction to Thermoelectricity. In.

2. Bian, Z.; Shakouri, A., Cooling Enhancement Using Inhomogeneous Thermoelectric Materials. In.

3. Vining, C. B., Semiconductors are cool. In *NATURE*, 2001; Vol. 413, pp 577-578.

4. Koumoto, K.; Terasaki, I.; Murayama, M., *Oxide Thermoelectrics*. Research Signpost: India, 2002.

5. Fairbanks, J., THERMOELECTRIC APPLICATIONS IN VEHICLES STATUS 2008. In.

6. Borisenko, V. E., *Semiconducting Silicides*. Springer: New York, 2000.

7. Yoshinaga, M.; Iida, T.; Noda, M.; Endo, T.; Takanashi, Y., Bulk crystal growth of Mg2Si by the vertical Bridgman method. *Thin Solid Films* **2004,** 461, 86-89.

8. Vining, C. B. In *THERMOELECTRIC FUNDAMENTALS AND PHYSICAL PHENOMENA*, Short Course On Thermoelectrics, Japan, 1993; The International Thermoelectric Society: Japan, 1993.

9. Zhu, Z. H.; Zhu, C., Thermodynamical Study of the Thermoelectric Effect for Magnesium Silicide. *J. Phys. Chem. A* **2007,** 111, 9362-9366.

10. Jensen, F., *Introduction to Computational Chemistry*. 2nd ed.; WILEY: New York, 2006.

11. Piela, L., *Ideas of Quantum Chemstry*. 1st ed.; Elsevier: New York, 2007.

12. Bonin, K. D.; Kresin, V. V., *Electric-Dipole Polarizabilities of Atoms, Molecules and Clusters*. World Scientific: London, 1997.

13. Tabor, D., *Gases, liquids and solids and other states of matter*. 3rd ed.; Cambridge University Press: Cambridge, 1991.

14. Kittel, C., *Introduction to Solid State Physics*. 8th ed.; WILEY: USA, 2005.

15. Wheatley, P. J., *The Determination of Molecular Structure*. Dover: New York, 1968.

16. Bottcher, C. J. F., *THEORY OF ELECTRIC POLARIZATION*. 2nd ed.; Elsevier: New York, 1973

17. Atkins, P.; Paula, J. d., *ATKINS' Physical Chemistry*. 7th ed.; Oxford University Press: Oxford, 2002.

18. Cioslowski, J., A New Population Analysis Based on Atomic Polar Tensors. *JOURNAL AMERICAN CHEMICAL SOCIETY* **1989,** 111, 8333-8336.

19. S. Millefiori, A. A., (Hyper)polarizability of chalcogenophenes C4H4X (X = 0, S, Se, Te) Conventional ab initio and density functional theory study. *Journal of Molecaular Structure (Theochem)* **1998,** 43 I 59-78.

20. Per-Olof Astrand, K. R., Kurt V. Mikkelsen,Trygve Helgaker,, Atomic Charges of the Water Molecule and the Water Dimer. *J. Phys. Chem. A* **1998,** 102, 7686-7691

21. Frank De Proft, J. M. L. M., Paul Geerlings,, On the performance of density functional methods for describing atomic populations, dipole moments and infrared intensities. *Chemical Physics Lette* **1996,** 250, 393-401

22. Michael Springborg, *Methods of Electronic-Structure Calculations From Molecules to Solid*. WILEY: New York, 2000.

23. Wolfram Koch, M. C. H., *A Chemist's Guide to Density Functional Theory*. Wiley-VCH: New York, 2001.

24. Yan Zhao, N. E. S., D. G. Truhlar, Exchange-correlation functional with broad accuracy for metallic and nonmetallic compounds, kinetics, and noncovalent interactions. *THE JOURNAL OF CHEMICAL PHYSICS* **2005,** 123, 161103.

25. Yan Zhao, N. E. S., Donald G. Truhlar, Design of Density Functionals by Combining the Method of Constraint Satisfaction with Parametrization for Thermochemistry, Thermochemical Kinetics, and Noncovalent Interactions. *J. Chem. Theory Comput.* **2006,** 2, 364-382.

26. Thomas Kent Reynolds. Design, Synthesis, and Characterization of New Materials for Thermoelectric Applications. Cornell University, United States, 2003.

27. Terry M.Tritt, M. A. S., Guest Editors, Thermoelectric Materials, Phenomena, and Applications: A Bird's Eye View. *MRS BULLETIN* **2006,** 31, 188-194.

28. G. S. Nolas, J. S., H. J. Goldsmid, *Thermoelectrics: Basic Principles and New Materials Developments*. Springer: New York, 2001.

29. David Michael Rowe, REVIEW THERMOELECTRIC WASTE HEAT RECOVERY AS A RENEWABLE ENERGY SOURCE. *International Journal of Innovations in Energy Systems and Power* **2006,** 1, 13-23.

30. Xie An-Dong, Y. S.-Y., Zhu Zheng-He,Fu Yi-Bei, Spin polarization effect for

Os2 molecule. *Chinese Physics* **2005,** 14, 1808-1812.

31.   Kevin M. Wedderburn, S. B., Mel Levy,Robert J. Gdanitz, Geometries and stabilities of 3d-transition metal-cation benzene complexes, M^+Bz_n (M = Sc-Cu, n=1,2). *Chemical Physics* **2006,** 326, 600-604.

32.   Masayasu Akasaka, T. I., Takashi Nemoto,Junichi Soga,Junichi Sato,Kenichiro Makino,Masataka Fukano,Yoshifumi Takanashi, Non-wetting crystal growth of Mg2Si by vertical Bridgman method and thermoelectric characteristics. *Journal of Crystal Growth* **2007,** 304, 196-201.

33.   Zhongwei Jiang, W. Z., Liqin Yan, Xinhuan Niu, Anisotropy of the Seebeck coefficient in Czochralski grown p-type SiGe single crystal. *Materials Science and Engineering B* **2005,** 119, 182–184.

34.   M. C. Bost, J. E. M., Optical properties of semiconducting iron disilicide thin films. *Journal of Applied Physics* **1985,** 58, 2696-2703.

35.   S. Sugihara, S. K., H. Katanahara,H. Suzuki,S. Mochizuki,R. Sekine, Doping Effect of Metal into Iron Disilicide on Electronic Structures and Thermoelectric Properties. In *18th International Conference on Thermoelectrics*, 1999; pp 577-580.

36.   The General Properties of Si, Ge, SiGe, SiO2 and Si3N4. In Virginia Semiconductor: 2002.